Composites Part B 139 (2018) 130–145

Contents lists available at ScienceDirect

Composites Part B

journal homepage: www.elsevier.com/locate/compositesb

Probabilistic crack bridge model reflecting random bond properties and elastic matrix deformation

M. Vořechovský[a,*], R. Rypl[a], R. Chudoba[b]

[a] Institute of Structural Mechanics, Brno University of Technology, Czech Republic
[b] Institute of Structural Concrete, RWTH Aachen University, Germany

ARTICLE INFO

Keywords:
Microstructure
Bond strength
Micromechanics
Pull-out strength
Modeling

ABSTRACT

A semi-analytical probabilistic model of an isolated composite crack bridge is presented in this paper. With the assumptions of heterogeneous fibrous reinforcement embedded in an elastic matrix the model is capable of evaluating the stress and strain fields in both fibers and matrix. In order to be applicable as a representative unit in models at higher scales, the micromechanical response of the composite crack bridge is homogenized by using a probabilistic approach. Specifically, the mean response of a crack bridge is obtained as the integral of the response of a single fiber over the domain of random variables weighted by their joint probability density function. This approach has been used by the authors in a recent publication describing a single crack bridge with rigid matrix. The main extension of the present crack bridge model is the incorporation of elastic matrix deformations and of boundary conditions restricting fiber debonding at the crack bridge boundaries. The latter extension is needed to reflect the effects of interactions with neighboring cracks within a tensile specimen with multiple cracks. The model is verified against three limiting cases with known analytical solutions (fiber bundle model, crack bridge with rigid matrix, mono-filament in elastic matrix) and is shown to be in exact conformity with all of these limiting cases.

1. Introduction

The toughening effect of fibers used as reinforcement in ceramics is well known [2,16,17,34,42]. Provided that the interfacial layer allows for debonding and sliding of the fibers along the matrix, the notch sensitivity, thermal shock resistance and fracture toughness of fibrous composites can be significantly increased. If matrices with rather low tensile strength (e.g. cement-based matrices in textile reinforced concrete, ECC or SHCC) are reinforced with high-strength ceramic or polymer fibers, the aim is not only to increase the toughness but also to achieve a favorable quasi-ductile tensile behavior and increase the strength [33,45,55,57]. The quasi-ductility is caused by multiple cracking of the matrix and fiber debonding. In general, these composites, which are the focus of the present article, can be called (quasi-) brittle-matrix composites (BMC).

If unidirectional BMCs loaded in tension are designed for structural applications, it is imperative that a large redistribution capacity is available before the ultimate failure due to localized fiber damage is achieved [2,3,18,29,50]. The whole process of the composite tensile response is accompanied by considerable stress redistributions both between and within the composite constituents [21,35,47,48,64]. The qualitative and quantitative characteristics of BMCs strongly depend not only on the material and geometric properties of the constituents and their interface [2,39,65,70], but also on the statistical variability of these properties [37,55,62].

In order to avoid expensive numerical calculations, which are often highly redundant, considerable effort has been devoted to the development of multiscale models that employ homogenization techniques. Caggiano et al. [8] recently proposed the use of zero-thickness interface elements to reproduce the complex influence of fibers on the cracking phenomena of the concrete/mortar matrix. The finite element method [65–67,69], shear-lag analysis [48,51,66], Green's function method [35,64,67] and the fiber bundle model with equal load sharing have been used (among others) in the past for the analysis of the microscale mechanics of RVEs (representative volume elements) in fibrous composites [4,19,27,30,32,58,71]. In Refs. [25,26], unidirectional laminates have been studied using analytical micromechanics (Mori-Tanaka method) with elasticity in combination with a detailed calculation of stresses at the fiber-matrix interface to determine maximum macroscopic far-field stress. With the RVEs, the behavior of larger scaled domains can be extrapolated using appropriate analytical or numerical methods that take into consideration the variability of the RVE

* Corresponding author.
E-mail address: vorechovsky.m@vut.cz (M. Vořechovský).

https://doi.org/10.1016/j.compositesb.2017.11.040
Received 9 May 2017; Received in revised form 23 October 2017; Accepted 27 November 2017

properties and the related size-effects. With ever growing computational performance, the trend in recent years has been pointing towards nanoscales. Molecular dynamics is now widely used for the simulation of defects, dislocations and their interactions [10,38,59,68] and quantum mechanics is being applied to obtain most accurate interatomic interactions from first principles [22,46].

The influence of fibers on the stress level at the onset of matrix cracking and criteria for crack propagation have been studied into detail e.g. in Refs. [6,9,36,41,43,44]. The present work focuses more on the detailed description of stress transfer from heterogeneous bundle of bridging fibers into elastic matrix.

The present model belongs to the category of fiber bundle models reflecting material heterogeneity using the statistical representation of selected material parameters. The major difference of the present model compared to the majority of existing models is the inclusion of random bond strength τ and fiber radius r which introduce heterogeneity into the reinforcement at the microscale. Although the problem of bond heterogeneity has been addressed e.g. in Refs. [7,24,31,62,70], its effect on the tensile response of multiply cracked unidirectional composites has not yet been thoroughly analyzed by a probabilistic model. In Ref. [7], the nonuniform stress state within a multifilament yarn in textile reinforced concrete was modeled by variable filament lengths bridging a matrix crack. The nonlinear behavior during yarn pullout from the cementitious matrix was then assumed to be due solely to ruptures of individual filaments and debonding was neglected.

The authors of the present article have published a new approach to the micromechanics of an isolated discrete crack bridged by heterogeneous fibers in Ref. [55]. The main conclusion of the publication was that a higher reinforcement heterogeneity reduces the crack bridge strength and increases its toughness, which was also observed experimentally in Ref. [62]. In the present article, the model previously introduced by the authors in Ref. [55] is extended through:

1) **the evaluation of the stress state of the matrix.** In composites with heterogeneous reinforcement, the debonded lengths of individual fibers are variable which results in a nonlinear effective bond-slip law and thus a nonlinear matrix strain profile in the vicinity of a crack bridge, see Fig. 1. Within the debonded zones, the matrix stress is lower than its far field value, and as a result further matrix cracks are less likely to occur here. These zones have been called 'shielded' [50], 'slip' [1] or 'ineffective' [20] or 'transmission' [29] lengths in the literature. The size and form of the matrix stress profile along the longitudinal axis in the vicinity of a crack bridge determine important composite properties like the crack density, crack widths, the overall form of the stress-strain response and the matrix fragment length distribution.
2) **the interaction of serially coupled crack bridges** which plays a significant role as the crack density in a multiply cracked composite grows. Interactions are utilized by setting restrictions on fiber debonding at the symmetry point between neighboring matrix cracks. These debonding restrictions dictate the tensile stiffness of crack bridges and are the cause for the strain-hardening behavior of multiply cracked fibrous composites with continuous reinforcement.

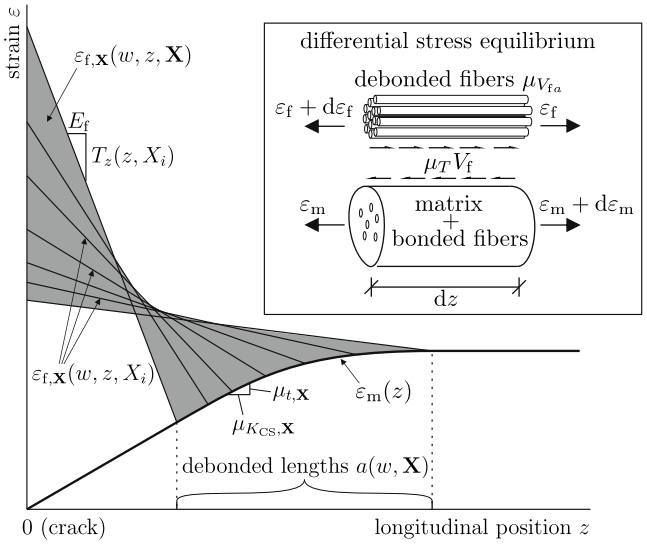

Fig. 1. Strain in fibers and matrix in the vicinity of a composite crack bridge: i denote realizations of fiber properties from the sampling space $\mathbf{X}$; differential equilibrium within a composite cross-section (frame).

Given these extensions, the representative crack bridge can be employed within a multiple cracking model [53,56] that utilizes e.g. the random strength approach as criterion for the stochastic crack initiation.

The paper is organized as follows: Sec. 2 introduces notation and the model assumptions. The model is derived in two steps: the probabilistic homogenization of the micromechanical response in Sec. 3 and the micromechanical formulation of a fiber bridging action. In order to verify the model's robustness, Sec. 5 provides three limiting cases with known analytical solutions and investigates the ability of the present model to reproduce them. Finally, conclusions and the demonstration of the effect of elastic deformation of matrix are drawn in Sec. 8.

2. Notation and assumptions

A single crack bridge in an unidirectional fiber reinforced composite with a constant cross-sectional area A_c and a volume fraction V_f of continuous fibers loaded in tension with the far field composite stress σ_c is considered. Both fibers and matrix are linear elastic with moduli of elasticity E_f and E_m, respectively, and the fibers fail in a brittle manner upon reaching their breaking strain ξ. This breaking strain refers to the fiber strain at the position of a matrix crack $\varepsilon_{\mathrm{f}0}$ (see Fig. 2). Fibers are assumed to have circular cross-section with radius r, cross-sectional area A_f and a constant frictional interface stress τ that equals the bond strength so that the bond vs. slip law is assumed to be ideally plastic with infinite initial stiffness. It follows that the terms bond stress and bond strength are interchangeable when this type of bond vs. slip law is used. This convenient assumption may be considered simplified. However, the authors argue that for fibers in brittle matrices, the selection of a constant interfacial shear stress is reasonable. The fibers typically have rather low bond to the matrix. When debonding at the interface occurs along part of the stress recovery region, shear stresses after debonding may be much lower than the shear stresses before debonding. However, these peaks get smoothed out as the frictional component can be surprisingly large. It is because the fiber fragments are, on average, very long and, also there are large normal stresses that can develop from the differential contraction of the fiber and matrix after elevated temperature curing and Poisson contraction effects due to tensile loading [34]. The initial elastic part of the bond-slip law is negligible and selection of the constant bond-slip law, used by most of authors, captures the essential nature of the stress recovery, see e.g. Ref. [34]. In cases of polymer matrices reinforced with fibers with much stronger bond to the matrix, a more complicated bond-slip law may be suitable [50,52]. The proposed crack bridge model is constructed such that it can act as a representative crack bridge within a tensile specimen with multiple cracks. The interaction between cracks is introduced by defining boundary conditions that reflect the stress symmetry between adjacent cracks bridges.

The strain is variable for individual fibers due to the parameters which affect the fiber-matrix bond and are assumed to be of a random nature. Due to the weak bond and high matrix stiffness characteristic of cement-based and ceramic matrix composites, only the longitudinal deformation of both fibers and matrix is considered and shear deformations [19,28,50] are ignored.

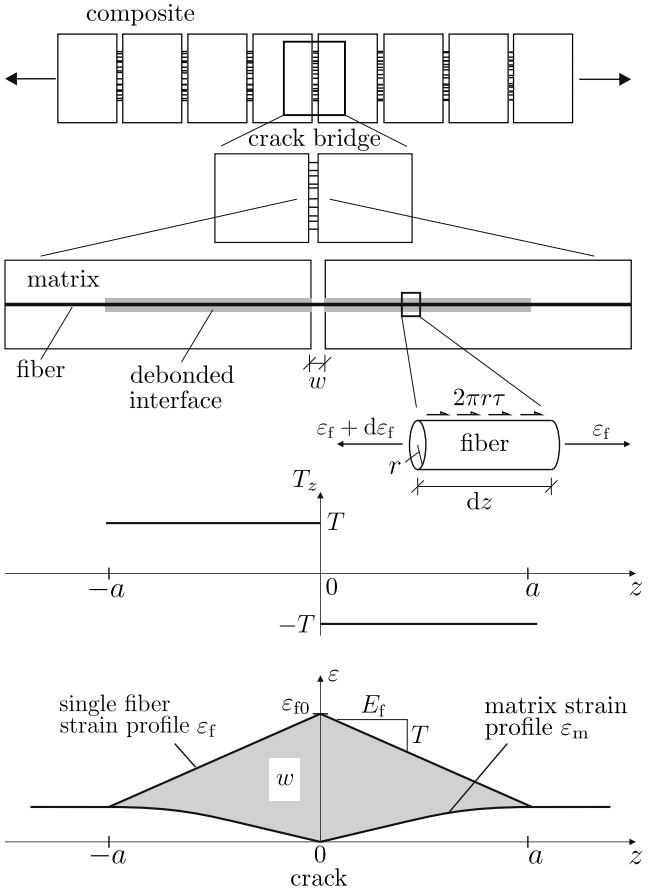

Fig. 2. Multi-scale modeling approach diagram.

The matrix crack is assumed to be planar and perpendicular to the loading direction. Any residual cohesive force transferred by the matrix crack planes is ignored so that the force is transmitted solely by the fibers. Between the crack planes, fibers bear the applied load and transmit it into the matrix along a debonded length a which depends on the constituent properties and the crack opening w so that

$$a = \mathscr{A}(w; \tau, r, E_m, E_f, V_f). \tag{1}$$

Throughout the paper, the parameters E_m, E_f and V_f are considered deterministic and the dependence on them is not explicitly stated in the equations. In the case of variable bond properties (heterogeneous reinforcement), the debonded length is a function of *random* bond and of the constituent properties. The idealization of the composite can be described as a set of parallel 1D springs (representing the fibers) with tensile stiffness per unit length $E_f A_f$ coupled to a single 1D spring (representing the matrix) with the stiffness $E_m A_c(1 - V_f)$ through a (possibly random) frictional bond with the shear flow per unit length $\ldots 2\pi r\tau$ An important deviation of the present model from the model with rigid matrix presented in Ref. [55] and from fiber-bundle models in general is the interaction of the fibers through the elastic matrix. Fibers are therefore not mechanically independent which has to be considered when their stress state is evaluated. It is implicitly assumed that fibers interact solely through the matrix and that a direct interaction via friction at the fiber-fiber interface does not take place. In Fig. 3a and Fig. 3b, the difference between independent and dependent fibers (through the elastic matrix) is shown in terms of fiber strain vs. crack opening and in Fig. 3c and 3d in terms of fiber strain along the fibers within a crack bridge.

Each gray line shows the response of a crack, bridged by a single fiber from the random domain with sampled parameters. Individual lines are obtained with a fiber parameter sampled from the probabilistic distribution of τ (samples are selected regularly with respect to probability – LHS sampling). The black lines in the top row of Fig. 3 represent an average response of the crack bridge reinforced by a bundle of fibers. They are obtained by computing the average fiber strain – an average from the responses for individual fibers for each value of the crack opening.

3. Homogenized composite response

It was explained in the course of the derivation of the crack bridge model with rigid matrix [55] that with the quasi-static crack opening w set as control variable, the composite stress can also be kept track of during the descending branch, while a force controlled model would only be able to track the stress up to its peak value (the existence of a descending branch implies that for a given force acting on the crack bridge, there exist more than one crack opening, see e.g. Fig. 4).

In Ref. [55], it was also stated that the crack opening equals the far field displacement u for rigid matrix. This statement is not true for the elastically deformable matrix (see Fig. 4). Depending on the fiber and matrix stiffness ratio and on the bond strength, the total displacement of a tensile specimen u will be equal or larger than the crack opening w. For some geometrical and stiffness configurations, the composite stress σ_c vs. u will exhibit snap-back behavior resulting in an unstable (dynamic) damage process. This behavior occurs, when energy release rate exceeded its critical value [5].

In such situations, the loading must be controlled by the crack-opening displacement w or by the energy release rate to ensure a stable loading process under all circumstances and to obtain a unique relation between the composite stress σ_c and total elongation u (see the dashed curve in Fig. 4). An example of the load control with monotonous influence of the control variable, w, on the response variable (pull-out force or composite stress, σ_c) is provided in Fig. 4 using the solid line.

In real experiments, however, controlling the loading by crack opening may be a difficult task and people tend to use loading controlled by the displacement of the loading platens. If there is a snap-back behavior related e.g. to an avalanche of ruptures of fibers, the displacement-controlled experiment is not able to track the whole snap-back curve, Fig. 4.

In composites with heterogeneous reinforcement individual fibers have variable properties and the composite stress is the normalized sum of their contributions to the bridging stress. It was derived in Ref. [55] that as the number of fibers n_f grows large, the normalized sum of all fiber responses converges by the law of large numbers to their average value. Thus, the composite response can be represented by the statistical average of many individual fibers.

Let the fiber strain at the matrix crack position be introduced as $\varepsilon_{f0,\mathbf{X}}(w, \mathbf{X})$ with w representing the crack opening and $\mathbf{X}$ standing for the sampling space of the assumed random variables. The resulting formula for the expected value of the composite stress σ_c (denoted as $\mu_{\sigma_c,\mathbf{X}}$) as a function of a nonnegative crack opening w is given as

$$\mu_{\sigma_c,\mathbf{X}}(w) = E_f V_f \mathrm{E}[\nu_f(r)\varepsilon_{f0,\mathbf{X}}(w, \mathbf{X})],\ w \geq 0, \tag{2}$$

where the average is denoted by the expectation operator $\mathrm{E}[\cdot]$ and the variable $\nu_f(r)$ is given by the expression

$$\nu_f(r) = \frac{r^2}{\mathrm{E}[r^2]} \tag{3}$$

and can be viewed as a weight factor for fibers with respect to their cross-sectional area (see Ref. [55] for details). The mean composite strength is defined as

$$\mu^{\star}_{\sigma_c,\mathbf{X}} = \sup\{\mu_{\sigma_c,\mathbf{X}}(w);\ w \geq 0\}. \tag{4}$$

We remark that Eqns. (2) and (4) are valid generally and thus hold also for the case of elastic matrix. In order to evaluate the mean values given by Eqns. (2) and (4), the fiber crack bridge function $\varepsilon_{f0,\mathbf{X}}(w, \mathbf{X})$

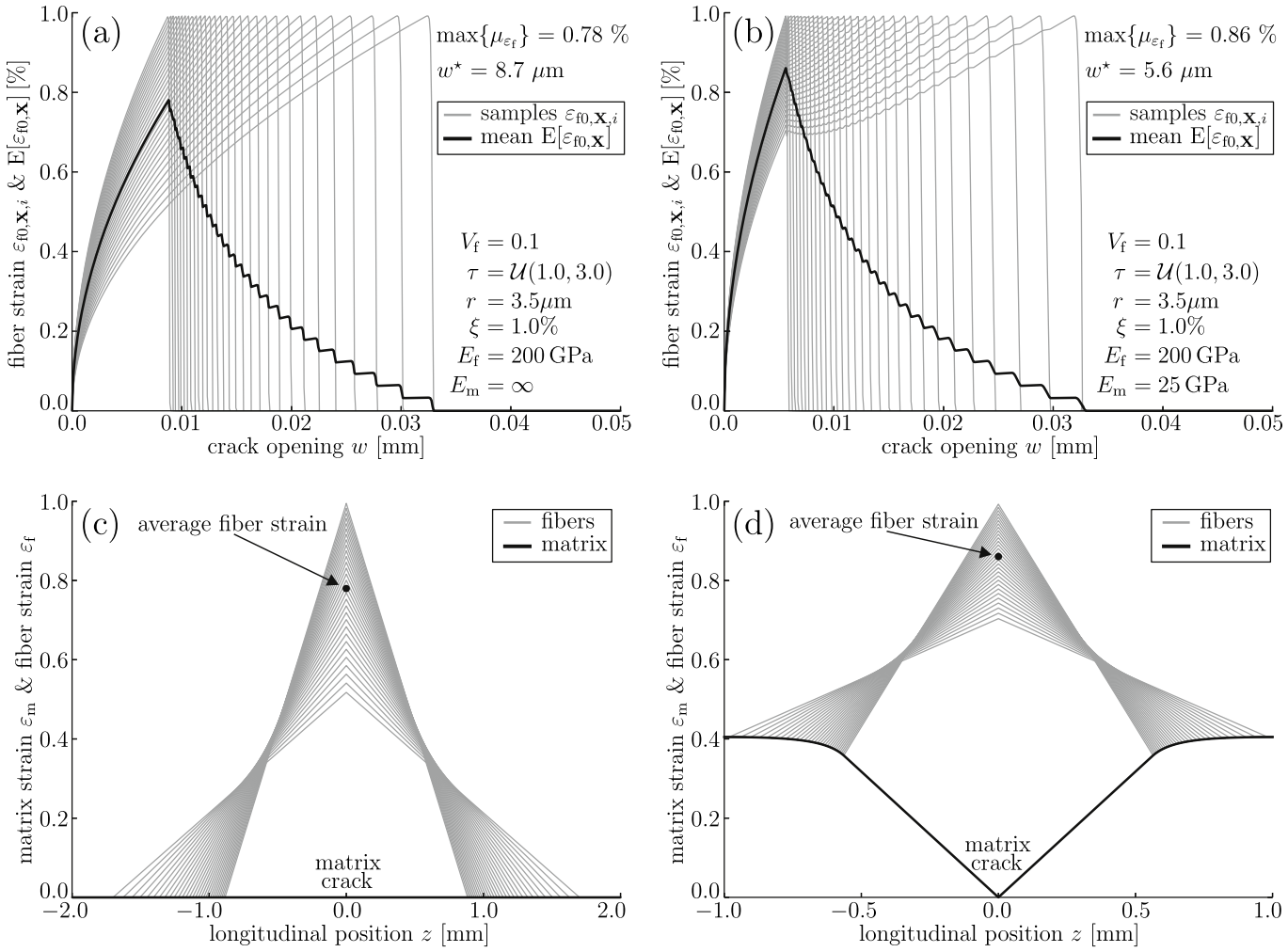

Fig. 3. Comparison of rigid matrix and elastic matrix: Fiber crack bridge function $\varepsilon_{f0,\mathbf{X},i}$ with $i = 1, \ldots, 30$ samples from $\mathbf{X}$ and their average value E[$\varepsilon_{f0,\mathbf{X}}$] considering (a) rigid matrix (b) elastic matrix; Fiber and matrix strain profiles along z considering (c) rigid matrix (d) elastic matrix. Bond strength τ is uniformly distributed between 1.0 N/mm^2 and 4.0 N/mm^2, i.e. the notation in the legend states $\mathcal{U}$(location, scale).

has to be resolved and the joint distribution function of the random variables must be provided [12,55].

The variance of the composite stress at a given crack opening was derived in Ref. [55] and explained to be decreasing inversely proportional to the increasing number of fibers. Daniels [23] has derived that the same rate applies for the variance of the composite strength. For practical structural scales, the theoretical variability of both the composite stress and strength stemming from randomness at the microscale is negligibly small. Note that there are other sources of randomness at the structural scale, which will cause variability in test results.

3.1. A note on the probabilistic approach

One may suggest to simplify the probabilistic approach by just 'evaluating the analytical model with average values of the random variables'. Such an approach would lead to incorrect conclusions because, in general, the expectation of a function of random variables does not equal the function of the expectations of the random variables, i.e.: $\mathrm{E}[f(\mathbf{X})] \neq f(\mathrm{E}[\mathbf{X}])$. The equality is only given for the special case of $f(\mathbf{X})$ being a linear combination of independent random variables. Since in the present model, we are dealing with interacting random variables governing nonlinear phenomena like fiber breakage and debonding, the probabilistic approach presented in this work is the only correct way to compute the effect of the random variables on the representative crack bridge response. In order to support our claim that using the average properties in the model to obtain the average response is inappropriate in the case of the crack bridge behavior, we present Fig. 5. In this example, the only random variable is the fiber breaking strain. Three values of variance of Weibullian random breaking strain are used while keeping the mean value identical. The line denoted as "deterministic" represents a response obtained with variance approaching zero, which equals the case of representing the random variable by its mean value. If the randomness of the breaking strain is taken into account and the average crack bridge response is evaluated correctly by probabilistic homogenization (as proposed in the present model) the resulting behavior differs qualitatively for each value of the breaking strain variance (response transition from brittle to ductile behavior, strength reduction for higher variance).

4. The fiber crack bridge function

To derive the 'fiber crack bridge function' in a straightforward way, we first assume that fibers have infinite strength and analyze the contribution of a single fiber within a composite crack bridge to the total transmitted stress. The aspect of finite fiber strength will be included at the very end of this section.

We assume the bond strength τ and the fiber radius r to be random variables so that the sampling space $\mathbf{X}$ spans two dimensions $\mathbb{R}^2$. These variables are orthogonal if no statistical dependence is assumed between the random variables.

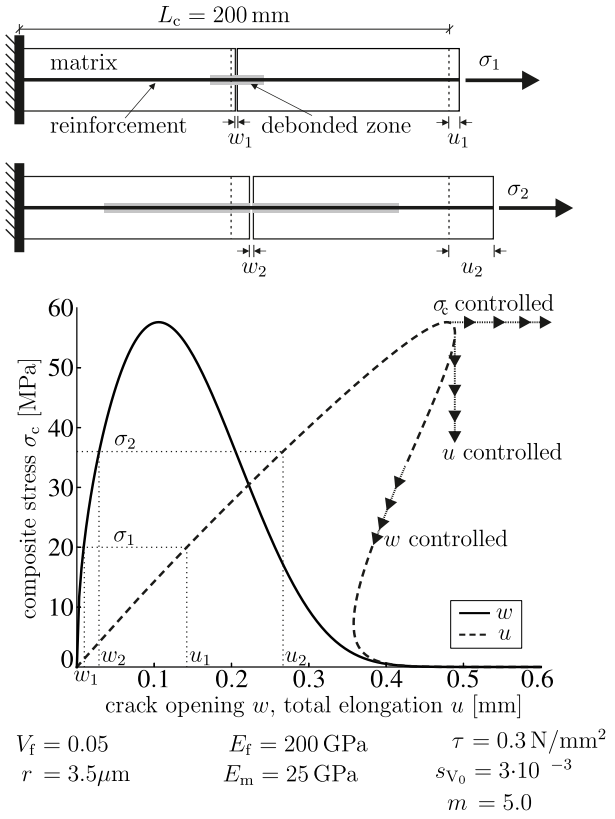

Fig. 4. Composite tensile specimen as controlled by the far field composite stress σ_c, displacement of the end point u and crack opening w.

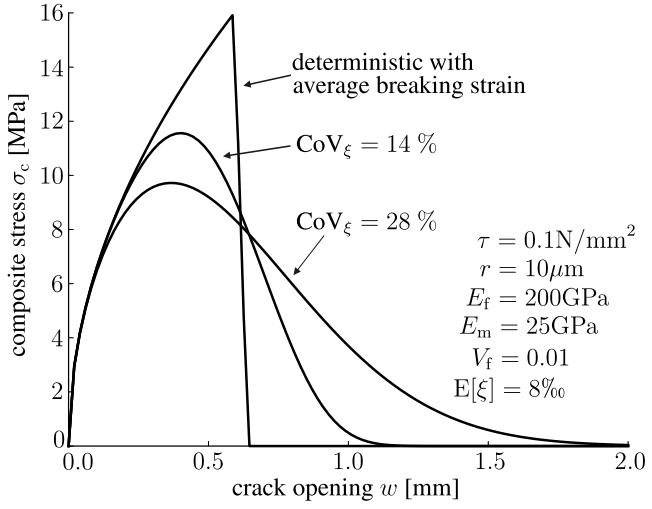

Fig. 5. Effect of spread of a random variable (breaking strain ξ) on the crack bridge performance in comparison with a deterministic approach.

The pullout of individual fibers from the matrix is simulated by the shear-lag model with infinite shear stiffness and a constant bond strength τ with constant frictional stress τ acting at the debonded interface [2,17,47]. When the far field stress σ_c is applied, the matrix crack opens by the amount w, the bridging fibers debond along the length a and transmit the force into the matrix. The transmitted force is a monotonic increasing function of the crack opening w, bond strength τ and the debonded length a, which depends on the random variables spanning the sampling space $\mathbf{X}$, i.e. $a = \mathscr{A}(w, \mathbf{X})$. For any debonded fiber, the differential equilibrium equation reads (see Fig. 2)

$$E_f \varepsilon'_{f,\mathbf{X}}(z) + T_z(z, \mathbf{X}) = 0, \tag{5}$$

with $\varepsilon'_{f,\mathbf{X}}(z)$ denoting the derivative of the fiber longitudinal strain $\varepsilon_{f,\mathbf{X}}(z)$ with respect to z:

$$\varepsilon'_{f,\mathbf{X}}(z) = \frac{d\varepsilon_{f,\mathbf{X}}(z)}{dz} = -\frac{T_z(z, \mathbf{X})}{E_f} \tag{6}$$

and $T_z(\mathbf{X}, z)$ the bond intensity given by

$$T_z(z, \mathbf{X}) = T(\mathbf{X}){\cdot}\mathrm{sign}(z). \tag{7}$$

Here, T is the shear flow per unit length normalized by the fiber cross-sectional area

$$T = \frac{2\pi r\tau}{\pi r^2} = \frac{2\tau}{r}. \tag{8}$$

In order to obtain the fiber strain at the crack plane, Eq. (6) is to be integrated. The resulting fiber strain profile $\varepsilon_{f,\mathbf{X}}$ along z has its maximum, $\varepsilon_{f0,\mathbf{X}}$, at the crack plane $z = 0$, and decays linearly with the distance from the crack with the slope $-T/E_f$.

4.1. Non-interacting crack bridges

Consider a crack bridge in which fibers can freely debond at both sides without restrictions. At the end point of debonded lengths, $z = \pm a$, the fiber strain is identical to the matrix strain, i.e. $\varepsilon_{f,\mathbf{X}}(z = \pm a) = \varepsilon_m(z = \pm a)$ (see Figs. 1 and 2). At distances $|z| \geq a$, the fiber strain equals the matrix strain $\varepsilon_m(z)$ so that fibers and matrix form a compact composite cross-section with a unique longitudinal strain shared by both constituents. The expression for the fiber strain within the debonded range is obtained by integrating Eq. (6) and taking into consideration the above mentioned boundary conditions

$$\varepsilon_{f,\mathbf{X}}(w, z, \mathbf{X}) = \varepsilon_m(-a) + \int_{-a}^{z} \varepsilon'_{f,\mathbf{X}}(x)dx \tag{9}$$

$$= \varepsilon_m(-a) + \frac{T(\mathbf{X})a - T_z(z, \mathbf{X})z}{E_f}, \quad |z| < a.$$

For the complete z domain, the fiber strain reads

$$\varepsilon_{f,\mathbf{X}}(w, z, \mathbf{X}) = \begin{cases} \varepsilon_m(a) + \frac{T(\mathbf{X})a - T_z(z,\mathbf{X})z}{E_f} & : |z| < a \\ \varepsilon_m(z) & : |z| \geq a \end{cases} \tag{10}$$

with $\varepsilon_m(-a) = \varepsilon_m(a)$ due to the symmetry of the fiber strain about the crack plane $z = 0$. Note that these formulas involve the debonded length a which is a function of w and $\mathbf{X}$ (see Fig. 1). The dimension of $\varepsilon_{f,\mathbf{X}}$ is thus $\mathbb{R}^{n+2}$, which corresponds to the $n = 2$ dimensions of the sampling space $\mathbf{X}$, the dimension of the longitudinal position z and of the crack opening w. By formulating the fiber crack bridge function as the maximum fiber strain at $z = 0$, i.e.

$$\varepsilon_{f0,\mathbf{X}}(w, \mathbf{X}) = \varepsilon_{f,\mathbf{X}}(w, z = 0, \mathbf{X}) = \varepsilon_m(a) + \frac{T(\mathbf{X})a}{E_f} \tag{11}$$

the dimensionality is reduced to $\mathbb{R}^{n+1}$.

There are two unknowns in Eq. (11): the debonded length a and the longitudinal matrix strain $\varepsilon_m(a)$. Note that for composites with a stiff matrix, $E_m(1 - V_f) \gg E_f V_f$, i.e. $\varepsilon_m(z) \approx 0$, both the debonded lengths a and the fiber crack bridge function $\varepsilon_{f0,\mathbf{X}}(w, \mathbf{X})$ are simple analytical functions of w and $\mathbf{X}$ [55]. However, if the matrix deformations are not negligible, individual fibers are interconnected and the evaluation of Eq. (11) is not trivial in general because it depends on the stress state of *all* fibers. A simple solution is only possible in special cases, see Sec. 5. To evaluate the unknowns a and $\varepsilon_m(a)$, we have to consider a differential equilibrium of stresses in the matrix with a kinematic constraint. The sought variables are then found as the solution of an initial value problem, which is discussed in the remainder of this subsection.

With the assumption of negligible shear deformations of the matrix (zero shear-lag thickness assumption), the differential equilibrium of matrix stresses in the longitudinal direction can be stated as

$$K_{cs}(z)\varepsilon'_m(z) - t(z) = 0, \tag{12}$$

where $\varepsilon'_m(z) = \mathrm{d}\varepsilon_m(z)/\mathrm{d}z$ is the derivative of the axial matrix strain with respect to z, $t(z)$ is the longitudinal traction originating from the friction of debonded fibers at the fiber-matrix interface and $K_{cs}(z)$ is the axial stiffness of the compact composite cross-section. It is to be explained that the compact composite stiffness $K_{cs}(z)$ includes the stiffness of both matrix and bonded fibers, i.e. fibers with zero slip at the position z. Considering the general case, where there are n_f fibers in the composite cross-section and they have variable debonded lengths due to their random properties, $K_{cs}(z)$ at a particular crack opening w (the dependency on w is not explicitly denoted in the following formulas) and at the distance z from the matrix crack is derived as

$$K_{cs}(z) = E_m A_m + E_f\left(A_{f,tot} - \sum_{i=1}^{n_f} A_{f,i}\cdot H(a_i - z)\right). \tag{13}$$

The longitudinal traction $t(z)$ at w and z is

$$t(z) = \sum_{i=1}^{n_f} T_i A_{f,i}\cdot H(a_i - z) \tag{14}$$

which equals the traction of the debonded fibers, i.e. fibers with $|z| < a_i$, see Fig. 2 bottom. The variables T_i, $A_{f,i}$ and $a_i = \mathscr{A}(w, X_i)$ are respectively the bond intensities, fiber cross-sectional areas and debonded lengths of individual fibers denoted by the subscripts $i = 1,2, ...,n_f$. These variables depend on random parameters which can be considered as sampling points X_i from the sampling space $\mathbf{X}$. The deterministic variables A_m and $A_{f,tot}$ are the matrix cross-sectional area and the total cross-sectional area of all n_f fibers, respectively. The function $H(\cdot)$ denotes the Heaviside step function defined as

$$H(x) = \begin{cases} 0 & : x < 0 \\ 1 & : x \geq 0. \end{cases} \tag{15}$$

The role of the Heaviside function in Eqns. (13) and (14) is to exclude bonded fibers from the summations. Assuming a large number of fibers, the sum in Eq. (13) can be approximated by statistical average as

$$\sum_{i=1}^{n_f} A_{f,i}\cdot H(a_i - z) \approx n_f \mathrm{E}[A_f\cdot H(a - z)] \tag{16}$$

and the sum in Eq. (14) can be approximated in a similar way as

$$\sum_{i=1}^{n_f} T_i A_{f,i}\cdot H(a_i - z) \approx n_f \mathrm{E}[TA_f\cdot H(a - z)]. \tag{17}$$

Substituting these expressions back into Eqns. (13) and (14) and relating these approximations of $K_{cs}(z)$ and $t(z)$ to a unit composite cross-sectional area provides the expressions for their mean, normalized values

$$\mu_{K_{cs},\mathbf{X}}(z) = \frac{E_m A_m}{A_c} + \frac{E_f}{A_c}(A_{f,tot} - n_f \mathrm{E}[A_f\cdot H(a - z)]) \tag{18}$$

and

$$\mu_{t,\mathbf{X}}(z) = \frac{n_f}{A_c}\mathrm{E}[TA_f\cdot H(a - z)]. \tag{19}$$

If A_c is now substituted by its asymptotic value for a large number of fibers as $A_c \approx n_f \mathrm{E}[A_f]/V_f$ (see Ref. [55] for the derivation) and the substitution given by Eq. (3) is applied, Eqns. (18) and (19) can be rewritten as

$$\mu_{K_{cs},\mathbf{X}}(z) = E_c - E_f V_f \mathrm{E}[\nu_f(r)\cdot H(a - z)] \tag{20}$$

and

$$\mu_{t,\mathbf{X}}(z) = V_f \mathrm{E}[T\nu_f(r)\cdot H(a - z)]. \tag{21}$$

with $E_c = E_m(1 - V_f) + E_f V_f$ being the composite stiffness given by the rule of mixtures. Substituting these expressions into the original differential equilibrium equation Eq. (12), the matrix strain derivative can be asymptotically expressed as

$$\varepsilon'_m(z) \approx \frac{\mu_{t,\mathbf{X}}(z)}{\mu_{K_{cs},\mathbf{X}}(z)}. \tag{22}$$

With the initial value of zero matrix strain at the crack position, $\varepsilon_m(0) = 0$, we have an initial value problem, the solution of which is the unknown matrix strain profile along z needed for the evaluation of the fiber crack bridge function Eq. (11).

However, the differential equation still includes the unknown debonded length of fibers a. The additional equation needed for solving the unknown a is a kinematic constraint of the crack bridge problem stating that the crack opening is identical for all fibers irrespective of their random parameters from the sampling space $\mathbf{X}$. The crack opening is defined as the difference between the fiber and matrix strains, integrated over the whole debonded range:

$$w = \int_{-a}^{a} \varepsilon_{f,\mathbf{X}}(\mathbf{X}, z) - \varepsilon_m(z)\mathrm{d}z \tag{23}$$

which implicitly includes the debonded length a and relates it to the control variable – the crack opening w. Note that for a particular sampling point (vector of random parameters) X_i from the sampling domain $\mathbf{X}$, the crack opening given by Eq. (23) can be interpreted as the shaded area in Fig. 2. With the substitution of the implicit expression for a given by Eq. (23) into Eq. (22), a 2nd order ODE is obtained which can be integrated using a suitable numerical method to yield the matrix strain profile $\varepsilon_m(z)$ and, particularly, its value at $\varepsilon_m(a)$ needed for the fiber crack bridge function given by Eq. (11).

The authors propose a method for solving the differential equation, which transforms it into a 1st order ODE with separable variables (see Appendix A) and provides a solution in closed form. The resulting formula for the matrix strain $\varepsilon_m(w, \varepsilon'_{f,\mathbf{X}})$ is written as a function of the crack opening w and the fiber strain derivative $\varepsilon'_{f,\mathbf{X}}$ (Eq. (6)), which directly links the matrix strain to the sampling space $\mathbf{X}$. The resulting $\varepsilon_m(w, \varepsilon'_{f,\mathbf{X}})$ equals the matrix strain at the position of the debonded length of a fiber with the strain derivative $\varepsilon'_{f,\mathbf{X}}$ and reads

$$\varepsilon_m(w, \varepsilon'_{f,\mathbf{X}}) = \int_{-\infty}^{\varepsilon'_{f,\mathbf{X}}} \varepsilon'_m \varepsilon'_f \frac{\mathrm{d}a(w, \varepsilon'_f)}{\mathrm{d}\varepsilon'_f}\mathrm{d}\varepsilon'_f \tag{24}$$

with the derivative

$$\frac{\mathrm{d}a(w, \varepsilon'_{f,\mathbf{X}})}{\mathrm{d}\varepsilon'_{f,\mathbf{X}}} = -\frac{a(w, \varepsilon'_{f,\mathbf{X}})}{2[|\varepsilon'_{f,\mathbf{X}}| + \varepsilon'_m(w, \varepsilon'_{f,\mathbf{X}})]} \tag{25}$$

and the debonded length given as

$$a(w, \varepsilon'_{f,\mathbf{X}}) = \sqrt{\exp[F(\varepsilon'_{f,\mathbf{X}})]w}, \tag{26}$$

where $F(\varepsilon'_{f,\mathbf{X}})$ is the antiderivative of the function

$$f(\varepsilon'_{f,\mathbf{X}}) = \frac{\mathrm{d}F(\varepsilon'_{f,\mathbf{X}})}{\mathrm{d}\varepsilon'_{f,\mathbf{X}}} = -\frac{1}{|\varepsilon'_{f,\mathbf{X}}| + \varepsilon'_m(\varepsilon'_{f,\mathbf{X}})}. \tag{27}$$

Having derived the debonded lengths of fibers $a(w, \varepsilon'_{f,\mathbf{X}})$ and the matrix strain $\varepsilon_m(w, \varepsilon'_{f,\mathbf{X}})$ (which equals $\varepsilon_m(a)$ in Eq. (11)) by solving the differential equilibrium Eq. (22) with the kinematic constraint Eq. (23), the fiber crack bridge function $\varepsilon_{f0,\mathbf{X}}(w, \mathbf{X})$ can be easily computed for an isolated crack by substituting these variables into Eq. (11).

4.2. Interacting crack bridges

Recalling that the actual goal of the probabilistic crack bridge model (PCBM) is the simulation of a unidirectional composite with multiple cracks in series [53,56], the PCBM has to be able to take into account the interaction of neighboring cracks. At low tensile loads, few cracks can be expected to have occurred and the debonded lengths of fibers are rather short, so cracks can be considered as mechanically independent. However, if the load increases, the crack density grows and so do the debonded lengths of crack bridging fibers. When the debonded lengths

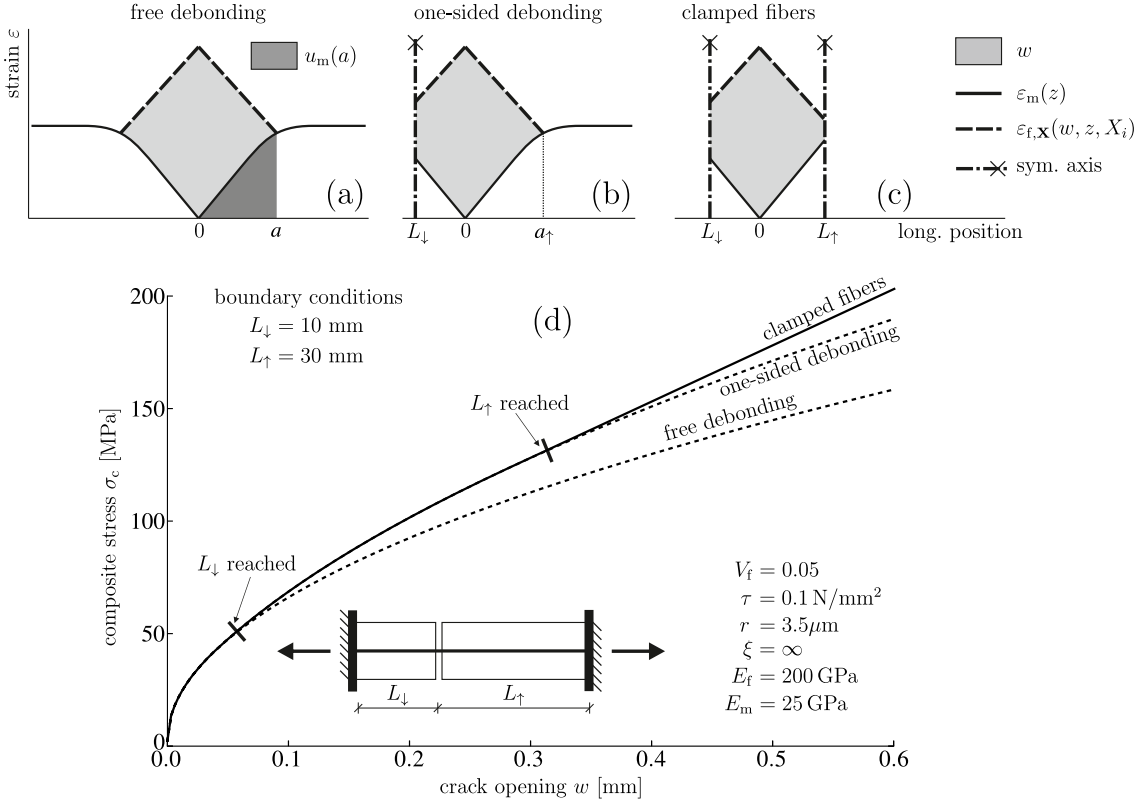

Fig. 6. Effect of boundary conditions on the fiber and matrix strain profiles (a–c). Composite crack bridge function with boundary conditions on fiber debonding (d).

of fibers from two neighboring cracks connect, further debonding is not possible and the fibers act as if they are clamped to the matrix at the point of connection of their debonded lengths – the fiber slip is restrained. The position of the contact between the debonded zones can be with reasonable accuracy assumed to be halfway between two adjacent cracks.

For the PCBM, the influence of neighboring cracks can thus be adapted as zero slip boundary condition on fibers. This reflects the stress symmetry between two cracks. In general, the distances to adjacent cracks at both sides of a particular crack are different. The half distance to the closer and more distant crack from the analyzed crack shall be denoted $L_\downarrow$ and $L_\uparrow$, respectively (see Fig. 6d).

When fibers debond up to the symmetry point between two cracks, the compliance of the crack bridge function grows slower with growing crack opening compared to free debonding on both sides. This is due to the fact that debonding only takes place on one side of the crack bridge where fibers are allowed to freely debond. As soon as all fibers debond up to the symmetry points on both sides of a crack, the crack bridge compliance becomes a constant with respect to further crack opening, with the result that the composite stress becomes a linear function of w (assuming that the damage of the constituents does not increase). In order to include the effect of boundary conditions, the fiber crack bridge function $\varepsilon_{f0,\mathbf{X}}(w, \mathbf{X})$, given by Eq. (11) for fibers with free debonding, has to be modified accordingly. Depending on the combination of adjacent crack distances and current debonded lengths, fibers can either be clamped to the matrix on one side and freely debond at the other side (Fig. 6b), or they have debonded up to the boundaries on both sides and thus behave as if they are clamped at both sides (Fig. 6c). These two cases are described in the following two subsections for fibers with assumed infinite strength.

4.2.1. One-sided debonding

Considering a single fiber that is clamped to the matrix on one side of the crack at the distance $L_\downarrow$ and freely debonds at the other side (see Fig. 6b), the corresponding kinematic constraint defining the crack opening (Eq. (23) for free debonding at both sides) has to be adapted as follows

$$w = \int_{-L_\downarrow}^{a_\uparrow} \varepsilon_{f,\mathbf{X}}(\mathbf{X}, z) - \varepsilon_m(z)\mathrm{d}z; \quad a(w, \varepsilon'_{f,\mathbf{X}}) > L_\downarrow. \tag{28}$$

If these debonded lengths $a(w, \varepsilon'_{f,\mathbf{X}})$, given by Eq. (26), exceed $L_\downarrow$, the kinematic constraint Eq. (28) applies and the crack opening is defined by the fiber and matrix strain difference integrated only within $-L_\downarrow$ and the debonded lengths $a_\uparrow$ of the one-sided debonding fibers.

The corresponding modification in the fiber crack bridge function, given by Eq. (11), affects only the function $a(w, \varepsilon'_{f,\mathbf{X}})$, which is now denoted as $a_\uparrow(w, \varepsilon'_{f,\mathbf{X}})$ for one-sided debonding. The full derivation is described in Appendix A and results in

$$a_\uparrow(w, \varepsilon'_{f,\mathbf{X}}) = \sqrt{2L_\downarrow^2 + \exp[F(\varepsilon'_{f,\mathbf{X}})]2w} - L_\downarrow. \tag{29}$$

4.2.2. Clamped fibers

As soon as the debonded lengths also reach $L_\uparrow$ – the half distance to the neighboring crack which is more distant (see Fig. 6c) – the kinematic constraint describing the crack opening becomes independent of the debonded length. It reflects a state in which no debonding is taking place, and has the following form

$$w = \int_{-L_\downarrow}^{L_\uparrow} \varepsilon_{f,\mathbf{X}}(\mathbf{X}, z) - \varepsilon_m(z)\mathrm{d}z; \quad a_\uparrow(w, \varepsilon'_{f,\mathbf{X}}) > L_\uparrow. \tag{30}$$

The fiber crack bridge function with this constraint has a different form than Eq. (11). It can be solved directly by integrating Eq. (30) and solving it for $\varepsilon_{f0,\mathbf{X}}$, which turns out to be a linear function of w (see Appendix A for the derivation)

$$\varepsilon_{f0,\mathbf{X}}(w, \mathbf{X}) = \frac{w + T/(2E_f)\left(L_\uparrow^2 + L_\downarrow^2\right) + u_m(L_\downarrow) + u_m(L_\uparrow)}{(L_\uparrow + L_\downarrow)}; \quad a_1(w, \varepsilon'_{f,\mathbf{X}}) > L_\uparrow \tag{31}$$

with $u_m(z)$ being the matrix longitudinal displacement relative to the crack position.

4.2.3. The general form with infinite fiber strength

If all possible boundary conditions are taken into account, the fiber crack bridge function can be expressed by the general formula

$$\varepsilon_{f0,\mathbf{X}}(w, \mathbf{X}, L_\downarrow, L_\uparrow) = \begin{cases} \text{Eq. (11)} & : 0 < \hat{a}(w, \varepsilon'_{f,\mathbf{X}}) < L_\uparrow \\ \text{Eq. (31)} & : L_\uparrow < \hat{a}(w, \varepsilon'_{f,\mathbf{X}}), \end{cases} \tag{32}$$

where

$$\hat{a}(w, \varepsilon'_{f,\mathbf{X}}) = \begin{cases} \text{Eq. (26)} & : 0 < a(w, \varepsilon'_{f,\mathbf{X}}) < L_\downarrow \\ \text{Eq. (29)} & : L_\downarrow < a(w, \varepsilon'_{f,\mathbf{X}}). \end{cases} \tag{33}$$

Note that since $\varepsilon_{f0,\mathbf{X}}$ is a function of $L_\downarrow$ and $L_\uparrow$, the dependency is also reflected in the matrix strain given by Eq. (24), i.e.

$$\varepsilon_m = \Sigma_m(w, \varepsilon'_{f,\mathbf{X}}, L_\downarrow, L_\uparrow). \tag{34}$$

4.2.4. Finite fiber strength

If fibers reach their breaking strain, ξ, they experience brittle failure and are assumed not to contribute to the total crack bridging force. As pointed out by various authors studying the strength of composites [20,50,60,63], broken fibers transmit a residual stress due to pullout. However, this effect is ignored in the present PCBM and fibers are assumed to break exactly at the crack plane. In other words, the ultimate value of the interface slip is marked by the breakage of the fiber. Quantitative results therefore represent a lower bound on strength and global toughness (the integral of the force over the crack opening).

For random breaking strain, the sampling domain has three dimensions corresponding to the three random variables $\mathbf{X} = \{\tau,\ r,\ \xi\}$. Using the Heaviside step function, the possibility of fiber rupture at the strain $\varepsilon_{f0} = \xi$ is introduced so that $\varepsilon_{f0,\mathbf{X}}$ is defined as

$$\varepsilon_{f0,\mathbf{X}}(w, \mathbf{X}) = \varepsilon_{f0}(w) \cdot H[\xi - \varepsilon_{f0}(w)], \tag{35}$$

where ε_{f0} is the strain at the crack plane of fibers with infinite strength. Fiber ruptures, depending on ε_{f0} and ξ, cause stress redistribution which influences the matrix strain state. Since ε_{f0}, on the other hand, depends on the matrix strain state as expressed in Eq. (11) for free debonding or by Eq. (32) in general, the formulation is implicit and ε_{f0} has to be computed iteratively.

The dependency of the matrix strain state on ε_{f0} is introduced by extending the differential equilibrium of matrix stress Eq. (22) by an additional Heaviside term in the variables $\mu_{K_{cs},\mathbf{X}}$ and $\mu_{t,\mathbf{X}}$, which takes fiber rupture into consideration. The evaluation of the compact composite stiffness then becomes

$$\mu_{K_{cs},\mathbf{X}}(z, \varepsilon_{f0}) = E_c - E_f V_{f,b,\xi}, \tag{36}$$

with

$$V_{f,b,\xi} = V_f \mathrm{E}[\nu_f(r) \cdot H(a - z) \cdot H(\xi - \varepsilon_{f0})] \tag{37}$$

where the additional Heaviside term $H(\xi - \varepsilon_{f0})$ ensures the addition of the fraction of broken fibers to the $\mu_{K_{cs},\mathbf{X}}(z)$ stiffness. Broken fibers are thus assumed to form a compact cross-section together with the matrix, on which the tractions of the intact debonded fibers are acting. Although the interaction of broken fibers with the matrix could be theoretically evaluated more precisely (e.g. in a similar fashion as proposed in Ref. [1] for the unloading stage of the hysteresis), the present simplification will not cause considerable inaccuracies. The mean longitudinal traction transmitted by fibers into the matrix $\mu_{t,\mathbf{X}}(z)$ (given by Eq. (21)) becomes, with the additional Heaviside term,

$$\mu_{t,\mathbf{X}}(z, \varepsilon_{f0}) = V_f \mathrm{E}[T\ \nu_f(r) \cdot H(a - z) \cdot H(\xi - \varepsilon_{f0})], \tag{38}$$

where $H(\xi - \varepsilon_{f0})$ ensures that only intact fibers contribute to the stress transmission. Having extended $\mu_{K_{cs},\mathbf{X}}(z, \varepsilon_{f0})$ and $\mu_{t,\mathbf{X}}(z, \varepsilon_{f0})$ by ε_{f0}, the matrix strain derivative, given by Eq. (22), becomes

$$\varepsilon'_m(z, \varepsilon_{f0}) = \frac{\mu_{t,\mathbf{X}}(z, \varepsilon_{f0})}{\mu_{K_{cs},\mathbf{X}}(z, \varepsilon_{f0})}. \tag{39}$$

The implicit formulation of ε_{f0} is therefore written as

$$\varepsilon_{f0}(w) = \varepsilon_m(a, \varepsilon_{f0}) + \frac{T}{E_f} a \tag{40}$$

for freely debonding fibers. For general boundary conditions on fiber debonding, Eq. (32) is applied with Eq. (39) substituted for the matrix strain derivative. The implicit Eq. (40) can be solved by using standard numerical algorithms and provides both ε_{f0} and ε_m. With these quantities, the crack bridge function can be solved in one simple step by substituting the evaluated ε_{f0} and ε_m into Eq. (35).

5. Model verification for limiting cases

The following sections demonstrate elementary examples of the mean composite crack bridge functions (Eq. (2)) with limiting values of particular parameters. These parameters are set in such a way that the model yields results for which an exact analytical solution is known. The analytical forms serve to verify the model. The following limiting cases are considered: fiber bundle model (Sec. 5.1); crack bridge with rigid matrix (Sec. 5.2); mono-filament in elastic matrix (Sec. 5.3).

5.1. The fiber bundle model

The strain based fiber bundle model describes the stress-strain behavior of a bundle of fibers with random strength. We show that this case is inherently included in the probabilistic crack bridge model (PCBM) when boundary conditions at finite distances $L_\downarrow$ and $L_\uparrow$ are set and the fiber breaking strain is assumed random. In particular, for the limiting case $\tau \to 0$, the PCBM reproduces the response of the strain based fiber bundle model.

5.1.1. Analytical solution

The analytical expression for the mean stress of a fiber bundle with random breaking strain was given e.g. in Refs. [15,49,54,61] as

$$\mu_{\sigma_b}(\varepsilon, L) = E_f \varepsilon [1 - G_\xi(\varepsilon, L)] \tag{41}$$

with $\varepsilon = u/L$ being the bundle strain (see Fig. 7), u the total

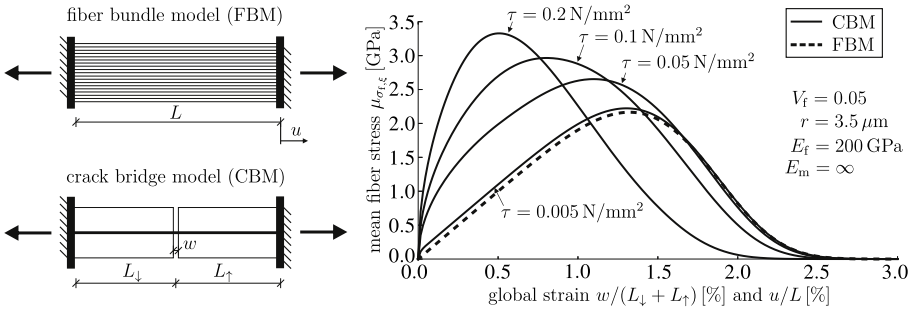

Fig. 7. Limiting behavior of the probabilistic crack bridge model as the bond strength decreases. The fiber strength has two-parameter Weibull distribution with shape = 5.0 and scale = 0.018.

displacement and $G_\xi(\varepsilon, L)$ the distribution of the fiber breaking strain at gauge length L.

5.1.2. Limit analysis of the PCBM

Under the conditions mentioned above, we study the behavior of the mean composite crack bridge function Eq. (2) divided by V_f yielding the mean fiber stress which shall be denoted as $\mu_{\sigma_f,\xi}$. The general form of $\mu_{\sigma_f,\xi}$ is

$$\mu_{\sigma_f,\xi}(w, \xi) = E_f \mathrm{E}[\varepsilon_{f0}(w) \cdot H[\xi - \varepsilon_{f0}(w)]] \tag{42}$$

with $\varepsilon_{f0}(w)$ being the fiber crack bridge function with infinite strength given by Eq. (35). As the bond strength approaches zero, the debonded lengths of fibers a and $a_\uparrow$ alike approach infinity for any value of $w > 0$. Since the boundary conditions $L_\downarrow$ and $L_\uparrow$ are finite, $\varepsilon_{f0}(w)$ is given by Eq. (31), which is the form of the fiber crack bridge function for $a_\uparrow > L_\uparrow$. Substituting $T = 2\tau/r = 0$ (zero bond strength), the equation simplifies to

$$\varepsilon_{f0}(w, \mathbf{X}) = \frac{w + u_m(L_\downarrow) + u_m(L_\uparrow)}{(L_\uparrow + L_\downarrow)}. \tag{43}$$

Because of the lack of interaction between fibers and matrix, the matrix displacements u_m vanish so that

$$\varepsilon_{f0}(w, \mathbf{X}) = \frac{w}{(L_\uparrow + L_\downarrow)}. \tag{44}$$

With zero matrix deformation, the crack opening w equals the total far field displacement u and Eq. (44) is the definition of constant tensile strain $\varepsilon = u/L$ of a dry fiber of length $L = L_\uparrow + L_\downarrow$. Substituting Eq. (44) into Eq. (42) and assuming the breaking strain of a fiber of the total length L to be distributed with $G_\xi(\varepsilon, L)$, where $\varepsilon = \varepsilon_{f0}$, the mean fiber stress yields

$$\begin{aligned}
\mu_{\sigma_f,\xi}(w, \xi) &= E_f \mathrm{E}[\varepsilon_{f0}(w) \cdot H[\xi - \varepsilon_{f0}(w)]] \\
&= E_f \varepsilon_{f0}(w) \int_{-\infty}^{\infty} H[\xi - \varepsilon_{f0}(w)] g_\xi(\varepsilon_{f0}, L) \mathrm{d}\xi \\
&= E_f \varepsilon_{f0}(w) \int_{\varepsilon_{f0}}^{\infty} g_\xi(\varepsilon_{f0}, L) \mathrm{d}\xi \\
&= E_f \varepsilon_{f0}(w)[1 - G_\xi(\varepsilon_{f0}, L)], \\
&= E_f \varepsilon_{f0}(w) \int_{-\infty}^{\infty} H[\xi - \varepsilon_{f0}(w)] g_\xi(\varepsilon_{f0}, L) \mathrm{d}\xi \\
&= E_f \varepsilon_{f0}(w) \int_{\varepsilon_{f0}}^{\infty} g_\xi(\varepsilon_{f0}, L) \mathrm{d}\xi \\
&= E_f \varepsilon_{f0}(w)[1 - G_\xi(\varepsilon_{f0}, L)],
\end{aligned} \tag{45}$$

with $g_\xi(\varepsilon_{f0}, L)$ being the density of the breaking strain at length L. This result proves the equivalence of the limiting case $\tau \to 0$ with the fiber-bundle model given by Eq. (41). Fig. 7 depicts the mean fiber stress obtained numerically using the PCBM and demonstrates convergence to the asymptotic fiber bundle model as τ decreases.

5.2. Crack bridge with rigid matrix

The crack bridge model with rigid matrix was derived in Ref. [55]. As the matrix stiffness increases, the predictions of the PCBM introduced in this paper will converge to those evaluated by the crack bridge model with rigid matrix. For the sake of simplicity, free debonding and infinite fiber breaking strain are assumed throughout the following derivation proving the convergence.

5.2.1. Analytical solution

With reference to [55], we recall that the mean composite crack bridge function for a crack bridge with rigid matrix is given by an equation that is identical to Eq. (2) in the present paper, but the single fiber function (when infinite fiber strength is assumed) has the form

$$\varepsilon_{f0,\mathbf{X}}(w, \mathbf{X}) = \sqrt{\frac{Tw}{E_f}}. \tag{46}$$

Since the homogenization of the composite stress in terms of mean values is identical for the present and the referenced model, it suffices to prove that $\varepsilon_{f0,\mathbf{X}}(w, \mathbf{X})$ given by Eq. (11) for the model with elastic matrix asymptotically converges to Eq. (46) as the matrix stiffness grows large.

5.2.2. Limit analysis of the PCBM

Eq. (11) defines the fiber crack bridge function for free debonding and elastic matrix in the form

$$\varepsilon_{f0,\mathbf{X}}(w, \mathbf{X}) = \varepsilon_m(a) + \frac{T(\mathbf{X})a}{E_f}. \tag{47}$$

The debonded length a is given by Eq. (26) as

$$a(w, \varepsilon'_{f,\mathbf{X}}) = \sqrt{\exp[F(\varepsilon'_{f,\mathbf{X}})]w}, \tag{48}$$

with $F(\varepsilon'_{f,\mathbf{X}})$ being the indefinite integral

$$F(\varepsilon'_{f,\mathbf{X}}) = -\int \frac{1}{|\varepsilon'_{f,\mathbf{X}}| + \varepsilon'_m(w, \varepsilon_{f,\mathbf{X}}')} \mathrm{d}\varepsilon'_{f,\mathbf{X}} \tag{49}$$

derived in Appendix A. With the same argumentation as above, the matrix strain derivative $\varepsilon'_m(w, \varepsilon_{f,\mathbf{X}}')$ becomes zero for infinitely stiff matrix so that

$$F(\varepsilon'_{f,\mathbf{X}}) = -\int \frac{1}{|\varepsilon'_{f,\mathbf{X}}|} \mathrm{d}\varepsilon'_{f,\mathbf{X}} = -\ln(|\varepsilon'_{f,\mathbf{X}}|). \tag{50}$$

With the substitution of Eq. (50) into Eq. (48), a can be evaluated as follows:

$$\begin{aligned}
a(w, \varepsilon'_{f,\mathbf{X}}) &= \sqrt{\exp[-\ln(|\varepsilon'_{f,\mathbf{X}}|)]w} \\
&= \sqrt{\frac{w}{|\varepsilon'_{f,\mathbf{X}}|}} = \sqrt{\frac{E_f w}{T}},
\end{aligned} \tag{51}$$

where the substitution given by Eq. (6) was used for $\varepsilon'_{f,\mathbf{X}}$. After substituting this expression into Eq. (47) and assuming zero matrix strain as its stiffness grows large, the fiber crack bridge function becomes

$$\varepsilon_{f0,\mathbf{X}}(w, \mathbf{X}) = \sqrt{\frac{Tw}{E_f}} \tag{52}$$

which equals Eq. (46) and completes the proof of the asymptotic behavior. Fig. 8 depicts numerically evaluated mean composite crack bridge functions demonstrating asymptotic convergence to the crack bridge model with rigid matrix as the matrix modulus of elasticity E_m increases. Unlike in the analytical derivation, the fiber strength was assumed finite and random in the numerical study. For the applied fiber-in-composite strength distribution, we refer to [55] and only give the parameters used for the study: Weibull modulus = 5.0; characteristic breaking strain = $6{\cdot}10^{-3}$ relative to the reference volume 1 mm^3.

5.3. Mono-filament in elastic matrix

The third limiting case is the crack bridge with elastic matrix and fibers with deterministic properties and infinite strength. This case has an analytical solution which is derived next, and the PCBM will be proved to yield this analytical solution for deterministic properties.

5.3.1. Analytical solution

For fibers with deterministic properties and infinite fiber strength, analytical solutions to $\varepsilon_m(a)$ and $\mu_{\sigma_c}(w)$, $w > 0$ exist. Considering free debonding at both sides of the crack, the stress state in the crack bridge is symmetric so that only the right hand side is analyzed in the following derivation. At a given crack opening w, all fibers have the same

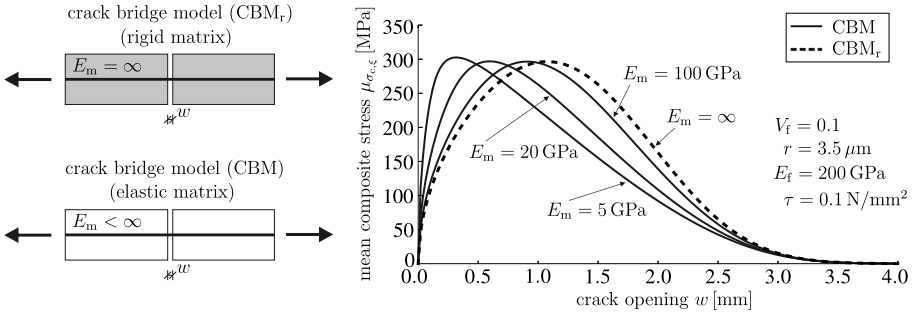

Fig. 8. Limiting behavior of the probabilistic crack bridge model as the matrix stiffness is increased.

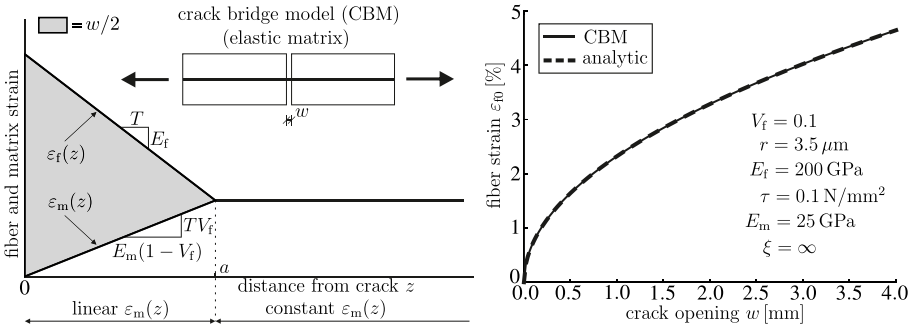

Fig. 9. Limiting behavior of the PCBM with deterministic parameters compared to the analytical solution.

debonded length a. The matrix strain in the range $z \in (0, a)$ is linear and so is the strain of all fibers, see Fig. 9. The slope of the fiber strain is defined by the force transmitted through the bond into the fiber per unit length, $-2\tau r\pi$ (with the minus sign because the fiber strain decreases with growing distance z from the matrix crack), divided by the fiber cross-sectional area πr^2 and by the modulus of elasticity E_f

$$\varepsilon_f'(z) = -\frac{2\tau r\pi}{\pi r^2 E_f} = -\frac{T}{E_f},\ z \in \left\langle 0, a \right\rangle. \tag{53}$$

The slope of the matrix strain up to a, where all fibers are debonded and transmit stress into the matrix, is given by

$$\varepsilon_m' = \frac{V_f T}{E_m(1 - V_f)},\quad z \in \left\langle 0, a \right\rangle \tag{54}$$

i.e. by the stress transfer $V_f T$ acting on a matrix which has the stiffness $E_m(1 - V_f)$. With the initial value $\varepsilon_m(0) = 0$, meaning zero matrix strain at the crack position, it can be directly integrated and results in a linear matrix strain within the debonded range (see Fig. 9)

$$\varepsilon_m(z) = \frac{V_f T}{E_m(1 - V_f)} z,\quad z \in \left\langle 0, a \right\rangle. \tag{55}$$

The integration of the fiber strain derivative $-T/E_f$ results in the fiber strain profile

$$\varepsilon_f(z) = \int \varepsilon_f'(z)\mathrm{d}z = \int -\frac{T}{E_f}\mathrm{d}z = -\frac{T}{E_f} z + C,\quad z \in \left\langle 0, a \right\rangle. \tag{56}$$

With the continuity condition $\varepsilon_m(a) = \varepsilon_f(a)$, the constant C is solved to be $C = \varepsilon_m(a) + Ta/E_f$, which substituted back into Eq. (56) results in

$$\varepsilon_f(z) = \varepsilon_m(a) + \frac{T(a - z)}{E_f},\quad z \in \left\langle 0, a \right\rangle. \tag{57}$$

The fiber strain at the crack position thus becomes

$$\varepsilon_{f0}(a) = \varepsilon_f(0) = \varepsilon_m(a) + \frac{Ta}{E_f}. \tag{58}$$

The remaining unknown – the debonded length a – can be solved by utilizing its connection to the control variable w through the integral in Eq. (23) that defines the crack width. With the substitution of Eq. (57) and Eq. (55) for $\varepsilon_{f,X}(z)$ and $\varepsilon_m(z)$, respectively, the integral (the shaded area in Fig. 9) has the form

$$\begin{aligned}\frac{w}{2} &= \int_0^a \varepsilon_{f,X}(z) - \varepsilon_m(z)\,\mathrm{d}z = \\ &= \int_0^a \varepsilon_m(a) + \tfrac{T(a-z)}{E_f} - \tfrac{V_f T}{E_m(1-V_f)} z\,\mathrm{d}z = \\ &= \left[\tfrac{TE_c}{2E_f E_m(1-V_f)}\right] a^2.\end{aligned} \tag{59}$$

The debonded length can now be solved as

$$a = \sqrt{\frac{E_f E_m(1 - V_f)w}{TE_c}}. \tag{60}$$

Substituting this expression for a in Eq. (58) results in the analytical form of the fiber crack bridge function:

$$\varepsilon_{f0}(w) = \sqrt{\frac{TE_c w}{E_f E_m(1 - V_f)}}. \tag{61}$$

5.3.2. Limit analysis of the PCBM

Since all parameters of the model are deterministic, the mean crack bridge response equals the fiber crack bridge function. Therefore, in order to prove the convergence of the model to the limiting case, it is sufficient to show the equivalence of the fiber crack bridge function given by Eq. (40) with the analytic expression Eq. (61).

Within the range $z \in (0, a)$, all fibers are debonded and transmit the stress $V_f T$ into the matrix, which has therefore a constant strain derivative in this interval. The debonded length as a constant for all fibers can in this case be evaluated by Eq. (26) as follows:

$$a(w, \varepsilon_f') = \sqrt{\exp[F(\varepsilon_f')]w} = \sqrt{\frac{w}{|\varepsilon_f'| + \varepsilon_m'}}, \tag{62}$$

where the integral $F(\varepsilon_f')$ can be directly solved as

$$F(\varepsilon_f') = -\int \frac{1}{|\varepsilon_f'| + \varepsilon_m'} d\varepsilon_f' = -\ln(|\varepsilon_f'| + \varepsilon_m') \tag{63}$$

because ε_m' is a constant with respect to ε_f' within the debonded length.[1] The matrix strain $\varepsilon_m(a)$ is evaluated by Eq. (24) with the substitution of Eq. (25) as

$$\varepsilon_m(a) = \int_{-\infty}^{\varepsilon_f'} -\frac{\varepsilon_m' a(w, \hat{\varepsilon}')}{2[|\hat{\varepsilon}'| + \varepsilon_m']} d\hat{\varepsilon}'. \tag{64}$$

By substituting Eq. (62) for $a(\hat{\varepsilon}')$ we obtain

$$\begin{aligned} \varepsilon_m(a) &= \int_{-\infty}^{\varepsilon_f'} -\sqrt{\frac{w}{|\hat{\varepsilon}'| + \varepsilon_m'}} \cdot \frac{\varepsilon_m'}{2[|\hat{\varepsilon}'| + \varepsilon_m']} d\hat{\varepsilon}' \\ &= -\frac{\varepsilon_m' \sqrt{w}}{2} \int_{-\infty}^{\varepsilon_f'} \frac{1}{[|\hat{\varepsilon}'| + \varepsilon_m']^{3/2}} d\hat{\varepsilon}' \end{aligned} \tag{65}$$

and after performing the integration

$$\int_{-\infty}^{\varepsilon_f'} \frac{1}{[|\hat{\varepsilon}'| + \varepsilon_m']^{3/2}} d\hat{\varepsilon}' = -\frac{2}{\sqrt{|\varepsilon_m'| + \varepsilon_m'}}, \tag{66}$$

the matrix strain becomes

$$\varepsilon_m(a) = \varepsilon_m' \sqrt{\frac{w}{|\varepsilon_f'| + \varepsilon_m'}} = \varepsilon_m' \, a, \tag{67}$$

where the last equality results from Eq. (62).

Now, it remains to evaluate the constants ε_f' and ε_m' by using Eqns. (6) and (22), respectively, as

$$\varepsilon_f' = -\frac{T}{E_f} \tag{68}$$

and

$$\varepsilon_m' = \frac{V_f T}{E_m(1 - V_f)}. \tag{69}$$

The fiber crack bridge function, Eq. (35), with substitutions of Eq. (67) for $\varepsilon_m(a)$ and Eq. (62) for a becomes

$$\varepsilon_{f0} = \varepsilon_m(a) + \frac{Ta}{E_f} = \varepsilon_m' \sqrt{\frac{w}{|\varepsilon_f'| + \varepsilon_m'}} + \sqrt{\frac{Tw}{E_f(|\varepsilon_f'| + \varepsilon_m')}} \tag{70}$$

and with the substitution of Eq. (68) for ε_f' and Eq. (69) for ε_m' its final form is obtained as

$$\varepsilon_{f0}(w) = \sqrt{\frac{TE_c w}{E_f E_m (1 - V_f)}}. \tag{71}$$

Hence the equality with Eq. (61) is given. This proves the ability of the model to reflect the analytical solution for this limiting case (see Fig. 9).

6. Effect of matrix elasticity

The present formulation of the model is based on the crack bridge model with rigid matrix introduced in Ref. [55] which is extended by the elastic deformation of the matrix. In order to demonstrate the effect of matrix elasticity, Fig. 10 depicts crack bridge strengths (solid lines) and corresponding crack openings (dashed lines) as functions of the fiber/matrix stiffness ratio.

Both the strength and the crack opening are normalized by their counterparts obtained with a rigid matrix. In general, the crack bridge strength increases with increasing matrix compliance. This effect is most pronounced for higher variability in bond variability. For a bond strength with a coefficient of variation 2.2, the strength increases by about 35% when the stiffnesses of fibers and matrix are of the same order. The strength increase can be explained by a stress homogenization among the fibers which is apparent when comparing Fig. 3c and 3d.

[1] For the general form of $F(\varepsilon_f')$ see Eq. (A.19).

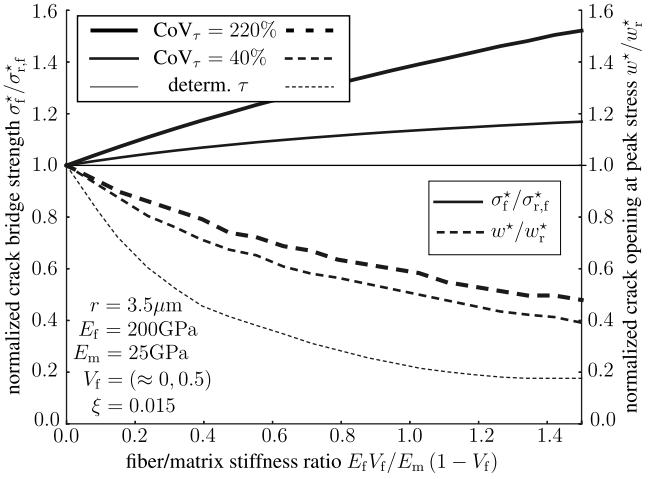

Fig. 10. Effect of matrix elasticity: Normalized crack bridge strengths and normalized crack openings at peak stress plotted over a range of fiber/matrix stiffness ratios. The bond strength is assumed to follow the Weibull distribution with scale 1.5 N/mm^2 and shapes {0.2, 3.0} (thicker lines) and deterministic value the 1.5 N/mm^2 (thin lines).

At the same time, the crack opening at peak stress decreases as the matrix stiffness decreases relative to the stiffness of the fibers. However, this effect is most pronounced when the properties are deterministic and diminishes with a growing bond variability. For a deterministic bond, the crack opening drops by about 75% when the fiber and matrix stiffness are of the same order. If the bond strength is variable with coefficient of variation 2.2, the crack opening at peak stresses decreases much slower over the studied range of fiber/matrix stiffnesses. This is because the homogenizing and strength increasing effect of the matrix elasticity leads to a much higher strength which goes along with a wider crack opening. We can speculate that for a theoretically very high scatter in bond strength, the crack opening at this peak stress could even increase with increasing fiber/matrix stiffness.

7. Model validation and parameter calibration

Model validation of the present PCBM at the level of a single crack bridge is difficult to realize. It is better to show the check the validity of the model at the level of multiple cracking as it occurs in the tensile test consisting of multiple crack bridges. Such a validation is left for a subsequent paper by the authors. Here, only a brief description of the procedure for calibration of model parameters is sketched.

The probabilistic distributions of the breaking strain, ξ, and radius of fibers, r, can be obtained using tensile tests on single filaments or eventually indirectly using tests on fiber bundles [13,14,61]. Once this is information is obtained, the probabilistic distribution of random bond properties (in this case the bond strength τ) can be obtained using notched tensile specimens, see the validation used for rigid matrix in Ref. [55]. The notched specimens behave like a single crack bridge and it is easy to control the embedded length of fibers and the related boundary conditions. Note that some authors propose to use single-fiber pull-out tests [11,40] for determination of bond properties. However, the parameters of heterogenous bond for reinforcing yarns used e.g. in textile reinforced concrete depend mostly on irregular penetration of the matrix into the yarns and therefore single-fiber pull-out tests are not representative. Even though the calibration of bond properties can be performed, a true validation of the present model considering elastic deformation of the matrix is only possible using tensile test on the whole composite specimens. Validation of the model involves not only the match between computed and measured effective stress-strain diagram, prediction of stress in deformed matrix but mainly correct prediction of the initiation and widths of cracks. Crack spacings and their widths may be critical parameters for durability considerations. In

the tensile experiment of the composite, parallel cracks progressively appear at weak locations and saturate the whole length of the composite. Their widths were measured by Digital Image Correlation system (Aramis).

In the model, these cracks can be represented by the crack bridges (PCBM) and they interact depending on the distances to adjacent cracks. The only parameters to calibrate are related to spatially variable random matrix strength. The subsequent paper introduces a model called Probabilistic Multiple Cracking Model (PMCM) and allows for validation of the present crack bridge model. Evaluation of the stress state in both composite constituents is necessary for the PCMC derived in the subsequent paper. The present probabilistic crack bridge model (PCBM) serves as a representative unit at the microscale within a multiscale model of strain hardening behavior of brittle matrix composites (PMCM). For this purpose, the interaction of adjacent crack bridges has been introduced into PMCM by setting boundary conditions on fiber debonding based on the assumption of stress symmetry between adjacent cracks.

8. Conclusions and discussion

The paper presents the derivation of a probabilistic crack bridge model (PCBM) of a composite with elastic-brittle matrix and heterogeneous fibrous reinforcement. It creates a link between the micromechanical formulation of a single fiber bridging action and the response of a multiply cracked composite specimen subjected to tensile loading where the PCBM can be used as representative crack bridge element.

- The single crack bridge behavior is represented by the homogenized response of individual fibers using a probabilistic homogenization approach suitable for a large number of parallel fibers.
- an earlier version of the model with a *rigid matrix* [55] is extended by the elastic deformation of the matrix. This extension allows for the evaluation of the stress state in both composite constituents, which is necessary for algorithms evaluating multiple cracking response of composites [53,56]. For this purpose, the interaction of adjacent crack bridges has been introduced by setting boundary conditions on fiber debonding based on the assumption of stress symmetry between adjacent cracks.
- The interconnection of the stress state of individual fibers through the elastic continuum of the matrix increases the complexity of the PCBM compared to the crack bridge model with *rigid matrix*. However, with the method the authors have introduced for the evaluation of the fibers-in-elastic-continuum problem (see Appendix A), the complexity is reduced to a reasonable level.
- The correctness of the model has been verified by comparing it to three limiting cases with known analytical solutions: 1) the fiber bundle model 2) a crack bridge with rigid matrix and 3) a monofilament in elastic matrix. It has been proved that the PCBM renders the limiting cases exactly.

Acknowledgments

This publication was supported by the Czech Science Foundation under the project no. 16-22230S, by the Czech Ministry of Education, Youth and Sports under project No. LO1408 “AdMaS UP - Advanced Materials, Structures and Technologies” under “National Sustainability Programme I” and by the German Federal Ministry of Education and Research (BMBF) as part of the Carbon Concrete Composite (C3) initiative, Project C-B3 and C3-V1.2. This support is gratefully acknowledged.

Appendix A. Matrix strain and debonded lengths

This appendix presents the derivation of the two unknowns in the fiber crack bridge function Eq. (11): the matrix strain $\varepsilon_{\mathrm{m}}(a)$ and the debonded length $a(w,\ \mathbf{X})$. The derivation is based on the differential equilibrium equation Eq. (22) and the kinematic constraint given by the crack opening Eq. (23).

With the assumption that fibers do not reach their strength, the sampling space includes two random variables $\mathbf{X} = \{\tau,\ r\}$. It has been derived in Sec. 4 that the derivative of the matrix strain at the position z is, for a large number of fibers, given by

$$\varepsilon'_{\mathrm{m}}(z) = \frac{\mu_{t,\mathbf{X}}(z)}{\mu_{K_{\mathrm{cs}},\mathbf{X}}(z)}. \tag{A.1}$$

The variable $\mu_{t,\mathbf{X}}(z)$ is the mean bond intensity, i.e. the mean value of the force transmitted by debonded fibers into the matrix, given by Eq. (21) and $\mu_{K_{\mathrm{cs}},\mathbf{X}}(z)$ is the mean compact composite stiffness given by Eq. (20). Both variables include the longitudinal position z in the Heaviside term. This ensures that the expected value is evaluated only for values from the sampling space $\mathbf{X}$ which satisfy the condition $a(\mathbf{X}) > z$. If $a(\mathbf{X}) < z$, the Heaviside function is zero and so is the contribution to the integral. However, the debonded length a is unknown beforehand so that the Heaviside term cannot be directly evaluated. A direct evaluation is only possible with a change of the control variable. Knowing that a increases monotonically with decreasing absolute value of the fiber strain derivative, $\varepsilon'_{\mathrm{f},\mathbf{X}}(\mathbf{X})$, given by Eq. (6), it can be taken as control variable in Eq. (A.1) with the notation $\varepsilon'_{\mathrm{f}}$. The new control variable $\varepsilon'_{\mathrm{f}}$ represents an iso-line in the sampling space $\mathbf{X} = \{\tau,\ r\}$ with constant values $T = 2\tau/r$. A higher absolute value of $\varepsilon'_{\mathrm{f}}$ corresponds to higher bond intensity which means that the debonded lengths are shorter and the corresponding peak strains higher (see Fig. 1). Eqns. (21) and (20) with $\varepsilon'_{\mathrm{f}}$ as control variable are redefined in the following way

$$\mu_{t,\mathbf{X}}(\varepsilon'_{\mathrm{f}}) = V_{\mathrm{f}}\ \mathrm{E}[T\ \nu_{\mathrm{f}}(r)\cdot H(\varepsilon'_{\mathrm{f},\mathbf{X}}(\mathbf{X}) - \varepsilon'_{\mathrm{f}})] \tag{A.2}$$

and

$$\mu_{K_{\mathrm{cs}},\mathbf{X}}(\varepsilon'_{\mathrm{f}}) = E_{\mathrm{m}}(1 - V_{\mathrm{f}}) + E_{\mathrm{f}}(V_{\mathrm{f}} - \mathrm{E}[\nu_{\mathrm{f}}(r)\cdot H(\varepsilon'_{\mathrm{f},\mathbf{X}}(\mathbf{X}) - \varepsilon'_{\mathrm{f}})]). \tag{A.3}$$

The unknown debonded length $a(\mathbf{X})$ in the Heaviside term was substituted by the fiber strain derivative $\varepsilon'_{\mathrm{f},\mathbf{X}}(\mathbf{X})$, a continuous function spanning the whole sampling space $\mathbf{X}$ given by Eq. (6), and the control variable z was substituted by $\varepsilon'_{\mathrm{f}}$. Note that the signs have to be switched.

Since the Heaviside terms in Eqn. (A.2) and (A.3) have the function of ‘cutting off’ the domain for integration by setting a part of it to zero, the same effect can be achieved by appropriately setting the integration ranges. This is utilized by performing the integration over the subspace $\hat{\mathbf{X}}$ of the sampling space $\mathbf{X}$ that satisfies the condition $|\varepsilon'_{\mathrm{f},\mathbf{X}}| > \varepsilon'_{\mathrm{f}}$

$$\mu_{t,\mathbf{X}}(\varepsilon'_{\mathrm{f}}) = \int_{\mathbf{X}} T\ \nu_{\mathrm{f}}(r) g_{r\tau}(r,\ \tau)\mathrm{d}\mathbf{X}, \tag{A.4}$$

and

$$\mu_{K_{cs},\mathbf{X}}(\varepsilon_f') = (1 - V_f)E_m + E_f\left[V_f - \int_{\mathbf{X}} \nu_f(r)\, g_{r\tau}(r, \tau)\mathrm{d}\mathbf{X}\right], \tag{A.5}$$

where $g_{r\tau}(r, \tau)$ is the joint probability density function of the two random variables τ and r. Eq. (A.1) with the substitution of Eqns. (A.4) and (A.5) becomes

$$\varepsilon_m'(\varepsilon_f') = \frac{\mathrm{d}\varepsilon_m(\varepsilon_f')}{\mathrm{d}z} = \frac{\mu_{t,\mathbf{X}}(\varepsilon_f')}{\mu_{K_{cs},\mathbf{X}}(\varepsilon_f')}, \tag{A.6}$$

which is the value of the matrix strain derivative with respect to z at the end debonded length of fibers with strain derivative ε_f'.

In order to obtain the matrix strain profile ε_m at a position z, its derivative ε_m' has to be integrated from 0 to z. With the change of the control variable to ε_f', the $\mathrm{d}z$ differential is substituted by

$$\mathrm{d}z = \frac{\mathrm{d}a}{\mathrm{d}\varepsilon_{f,\mathbf{X}}'}\mathrm{d}\varepsilon_{f,\mathbf{X}}' \tag{A.7}$$

(note that a has the same dimension as z) and the integration is performed from $-\infty$ to ε_f'.

$$\varepsilon_m(w, \varepsilon_f') = \int_{-\infty}^{\varepsilon_f'} \varepsilon_f'(\varepsilon_{f,\mathbf{X}}')\frac{\mathrm{d}a(w, \varepsilon_{f,\mathbf{X}}')}{\mathrm{d}\varepsilon_{f,\mathbf{X}}'}\mathrm{d}\varepsilon_{f,\mathbf{X}}'. \tag{A.8}$$

This relates the variable a to $\varepsilon_{f,\mathbf{X}}'$. Note that the fiber with infinite strain slope $\varepsilon_{f,\mathbf{X}}' = -\infty$ corresponds to an infinitely short debonded length $a = 0$. The derived equation solves the first unknown in the fiber crack bridge function – the matrix strain value – but only as controlled by the fiber strain derivative. To fully solve the problem, the relation between the debonded length a and the fiber strain derivative $\varepsilon_{f,\mathbf{X}}'$ is further needed.

The differential in Eq. (A.8) is derived below in course of the evaluation of the second unknown, the debonded length a as a function of $\varepsilon_{f,\mathbf{X}}'$. Since the definition of $a(\varepsilon_{f,\mathbf{X}}')$ depends on the boundary conditions for the debonding of fibers (see Fig. 6), it is derived for the respective cases separately in the following sections.

Appendix A.1. Free debonding

If fibers are allowed to freely debond, i.e. their debonding is not restraint due to interaction with a neighboring crack, the strain fields are symmetrical about the crack plane so that only one half of the filed can be considered (see Fig. 6a). In the following, the positive half-space is considered (positive z values). Without loss of generality, Eq. (23), which defines the crack opening as the integrated difference between the fiber and matrix strain, can be written in the form

$$\frac{w}{2} = \int_0^a \varepsilon_{f,\mathbf{X}}(z) - \varepsilon_m(z)\mathrm{d}z = \frac{|\varepsilon_{f,\mathbf{X}}'|a^2}{2} + \varepsilon_m(a)a - u_m(a), \tag{A.9}$$

where $\varepsilon_{f,\mathbf{X}}(z)$ and $\varepsilon_m(z)$ are the fiber and matrix strain, respectively, and $u_m(z)$ is the longitudinal matrix displacement given by the integration of ε_m along z.

In order to obtain the function $a(\varepsilon_{f,\mathbf{X}}')$ which assigns debonded lengths to fibers with strain slope $\varepsilon'_{f,\mathbf{X}}$, Eq. (A.9) is differentiated with respect to $\varepsilon_{f,\mathbf{X}}'$:

$$\frac{\mathrm{d}w}{\mathrm{d}\varepsilon_{f,\mathbf{X}}'} = \frac{\mathrm{d}|\varepsilon_{f,\mathbf{X}}'|a^2}{2\mathrm{d}\varepsilon_{f,\mathbf{X}}'} + \frac{\mathrm{d}\varepsilon_m(a)a}{\mathrm{d}\varepsilon_{f,\mathbf{X}}'} - \frac{\mathrm{d}u_m(a)}{\mathrm{d}\varepsilon_{f,\mathbf{X}}'}, \tag{A.10}$$

which, after applying the chain rule for derivatives and changing the control variable of $\varepsilon_m(a)$ to $\varepsilon_m(\varepsilon_{f,\mathbf{X}}')$, yields

$$0 = \frac{a^2}{2} + \left|\varepsilon_{f,\mathbf{X}}'\right|\frac{\mathrm{d}a}{\mathrm{d}\varepsilon'_{f,\mathbf{X}}}a + \varepsilon_m'(\varepsilon_{f,\mathbf{X}}')\frac{\mathrm{d}a}{\mathrm{d}\varepsilon_{f,\mathbf{X}}'}a. \tag{A.11}$$

This equation solved for $\mathrm{d}a/\mathrm{d}\varepsilon_{f,\mathbf{X}}'$ results in

$$\frac{\mathrm{d}a(w, \varepsilon_{f,\mathbf{X}}')}{\mathrm{d}\varepsilon_{f,\mathbf{X}}'} = -\frac{a(w, \varepsilon_{f,\mathbf{X}}')}{2[|\varepsilon_{f,\mathbf{X}}'| + \varepsilon'_m(\varepsilon_{f,\mathbf{X}}')]}, \tag{A.12}$$

which corresponds to the differential change of the debonded length a that goes along with a differential change in $\varepsilon_{f,\mathbf{X}}'$. Since it is a differential equation in separable form, it can be directly integrated in the following way: Eq. (A.12) is written in the form

$$\frac{\mathrm{d}a}{\mathrm{d}\varepsilon_{f,\mathbf{X}}'} = f(\varepsilon_{f,\mathbf{X}}')g(a) \tag{A.13}$$

with

$$f(\varepsilon_{f,\mathbf{X}}') = -\frac{1}{|\varepsilon_{f,\mathbf{X}}'| + \varepsilon_m'(\varepsilon_{f,\mathbf{X}}')} \tag{A.14}$$

and

$$g(a) = \frac{a}{2}. \tag{A.15}$$

Derived from Eq. (A.13), the following equality can be stated

$$\frac{1}{g(a)}\mathrm{d}a = f(\varepsilon'_{\mathrm{f,x}})\mathrm{d}\varepsilon'_{\mathrm{f,x}}. \tag{A.16}$$

Integrating both sides results in

$$G(a) = F(\varepsilon'_{\mathrm{f,x}}) + C \tag{A.17}$$

where $G(a)$ is the antiderivative of $1/g(a)$

$$G(a) = 2\ln(a) \tag{A.18}$$

and $F(\varepsilon'_{\mathrm{f,x}})$ is the antiderivative of $f(\varepsilon'_{\mathrm{f,x}})$

$$F(\varepsilon'_{\mathrm{f,x}}) = \int f(\varepsilon'_{\mathrm{f,x}})\mathrm{d}\varepsilon'_{\mathrm{f,x}}. \tag{A.19}$$

The solution to $a(\varepsilon'_{\mathrm{f,x}})$ is then obtained by substituting Eq. (A.18) into Eq. (A.17) and solving it for a as

$$a(\varepsilon'_{\mathrm{f,x}}) = G^{-1}(F(\varepsilon'_{\mathrm{f,x}}) + C) = \exp\left(\frac{F(\varepsilon'_{\mathrm{f,x}}) + C}{2}\right) \tag{A.20}$$

with the unknown constant C. The constant can be evaluated by stating that for $\varepsilon_{\mathrm{f,x}}{}' \to -\infty$ (fibers with an infinite strong bond), the debonded length will approach 0 and can be in the limit described by the formula

$$a(\varepsilon'_{\mathrm{f,x}} \to -\infty) = \sqrt{\frac{w}{|\varepsilon'_{\mathrm{f,x}}| + \varepsilon'_{\mathrm{m}}}}. \tag{A.21}$$

The reasoning behind this statement is that close to the matrix crack ($z = 0$), the matrix strain can be assumed linear and its derivative constant, which simplifies the relation between the debonded length and the crack opening w to the above equation (see Eq. (62) in Sec. 5 (limit case 'mono-filament in elastic matrix') for derivation). The function $F(\varepsilon'_{\mathrm{f,x}})$, with the assumption of constant matrix strain derivative is

$$F(\varepsilon'_{\mathrm{f,x}} \to -\infty) = \int f(\varepsilon'_{\mathrm{f,x}})\,\mathrm{d}\varepsilon'_{\mathrm{f,x}} = -\ln(|\varepsilon'_{\mathrm{f,x}}| + \varepsilon'_{\mathrm{m}}). \tag{A.22}$$

Substituting Eqns. (A.21) and (A.22) into Eq. (A.20) yields

$$\sqrt{\frac{w}{|\varepsilon'_{\mathrm{f,x}}| + \varepsilon'_{\mathrm{m}}}} = \exp\left(\frac{-\ln(|\varepsilon'_{\mathrm{f,x}}| + \varepsilon'_{\mathrm{m}}) + C}{2}\right), \tag{A.23}$$

which solves the constant C as

$$C = \ln(w). \tag{A.24}$$

The resulting form of a for fibers with free debonding as a function of the crack opening w and $\varepsilon'_{\mathrm{f,x}}$ is then

$$\begin{aligned} a(w, \varepsilon'_{\mathrm{f,x}}) &= \exp\left(\frac{F\left(\varepsilon'_{\mathrm{f,x}}\right) + \ln(w)}{2}\right) \\ &= \sqrt{\exp[F(\varepsilon'_{\mathrm{f,x}})]w}. \end{aligned} \tag{A.25}$$

This solves the second unknown in the fiber crack bridge function Eq. (11) for fibers with free debonding.

Appendix A.2. One-sided debonding

Fibers that have debonded up to the half distance $L_{\downarrow}$ between adjacent cracks at one side of the analyzed crack can further only debond at the other side of the crack with debonded length that are denoted as $a_{\uparrow}$ for the one sided debonding. The kinematic constraint for such fibers changes to Eq. (28) and corresponds to the shaded area in Fig. 6b. Note that in this case, the stress profiles are not symmetrical about the crack plane. Similar to free debonding, this kinematic constraint can be written as

$$\begin{aligned} w = &\left|\varepsilon'_{\mathrm{f,x}}\right|\left(\left(\frac{a_{\uparrow}^2}{2} + L_{\downarrow}a_{\uparrow} - \frac{L_{\downarrow}^2}{2}\right)+\right. \\ &\left. + \varepsilon_{\mathrm{m}}(a_{\uparrow})(a_{\uparrow} + L_{\downarrow}) - u_{\mathrm{m}}(a_{\uparrow}) - u_{\mathrm{m}}(L_{\downarrow})\right. \end{aligned} \tag{A.26}$$

and differentiated with respect to $\varepsilon'_{\mathrm{f,x}}$, which results in

$$0 = \left(\frac{a_{\uparrow}^2}{2} + L_{\downarrow}a_{\uparrow} - \frac{L_{\downarrow}^2}{2}\right) + \frac{\mathrm{d}a_{\uparrow}}{\mathrm{d}\varepsilon'_{\mathrm{f,x}}}(a_{\uparrow} + L_{\downarrow})(|\varepsilon'_{\mathrm{f,x}}| + \varepsilon'_{\mathrm{m}}). \tag{A.27}$$

Solving this equation for $\mathrm{d}a_{\uparrow}/\mathrm{d}\varepsilon'_{\mathrm{f,x}}$ results in

$$\frac{\mathrm{d}a_{\uparrow}(w, \varepsilon'_{\mathrm{f,x}})}{\mathrm{d}\varepsilon'_{\mathrm{f,x}}} = -\frac{a_{\uparrow}^2(w, \varepsilon'_{\mathrm{f,x}}) + 2a_{\uparrow}(w, \varepsilon'_{\mathrm{f,x}})L_{\downarrow} - L_{\downarrow}^2}{2(|\varepsilon'_{\mathrm{f,x}}| + \varepsilon'_{\mathrm{m}})(a_{\uparrow}(w, \varepsilon'_{\mathrm{f,x}}) + L_{\downarrow})}. \tag{A.28}$$

(with explicit notation of the functional dependencies). The result is separable so that it can be directly integrated analogically to the section above with the only difference that $g(a)$ now becomes

$$g(a_\uparrow) = \frac{a_\uparrow^2 + 2a_\uparrow L_\downarrow - L_\downarrow^2}{2(a_\uparrow + L_\downarrow)} \tag{A.29}$$

and the antiderivative of $1/g(a_\uparrow)$ is solved analytically as

$$G(a_\uparrow) = \ln(a_\uparrow^2 + 2a_\uparrow L_\downarrow - L_\downarrow^2). \tag{A.30}$$

The solution of

$$G(a_\uparrow) = F(\varepsilon'_{\mathrm{f},\mathbf{X}}) + C_1 \tag{A.31}$$

for the debonded length a is obtained by inverting $G(a_\uparrow)$ as

$$\begin{aligned} a_\uparrow(\varepsilon'_{\mathrm{f},\mathbf{X}}) &= G^{-1}(F(\varepsilon'_{\mathrm{f},\mathbf{X}}) + C_1) = \\ &= \sqrt{2L_\downarrow^2 + \exp[F(\varepsilon'_{\mathrm{f},\mathbf{X}}) + C_1]} - L_\downarrow. \end{aligned} \tag{A.32}$$

In order to find the unknown C_1, the continuity condition for debonded lengths of double sided and one sided debonding at the transition length $L_\downarrow$ is applied. Thus, $F(\varepsilon'_{\mathrm{f},\mathbf{X}})$ which solves the equation $a = L_\downarrow$ is calculated using Eq. (A.25) as

$$L_\downarrow = \sqrt{\exp[F(\varepsilon'_{\mathrm{f},\mathbf{X}})]w} \rightarrow F(\varepsilon'_{\mathrm{f},\mathbf{X}}) = \ln(L_\downarrow^2/w). \tag{A.33}$$

This expression substituted into Eq. (A.32) must solve also the equation $a_\uparrow = L_\downarrow$, which reveals the constant C_1 as

$$\begin{aligned} L_\downarrow &= \sqrt{2L_\downarrow^2 + \exp[\ln(L_\downarrow^2/w) + C_1]} - L_\downarrow \\ 2L_\downarrow^2 &= \exp(\ln(L_\downarrow^2/w) + C_1) \\ C_1 &= \ln(2w). \end{aligned} \tag{A.34}$$

This substituted into Eq. (A.32) provides the formula for debonded lengths $a_\uparrow$ for one-sided debonding as a function of the crack opening w and $\varepsilon'_{\mathrm{f},\mathbf{X}}$

$$a_\uparrow(w, \varepsilon'_{\mathrm{f},\mathbf{X}}) = \sqrt{2L_\downarrow^2 + \exp[F(\varepsilon'_{\mathrm{f},\mathbf{X}})]2w} - L_\downarrow. \tag{A.35}$$

Appendix A.3. Clamped fibers

For fibers, which are debonded at both sides of the crack up to the boundaries at distances $L_\downarrow$ and $L_\uparrow$, the kinematic constraint (the crack opening) is defined by Eq. (30), which is the shaded area in Fig. 6c. Performing the integration, the following form is obtained

$$w = (L_\uparrow + L_\downarrow)\varepsilon_{\mathrm{f0},\mathbf{X}} - \frac{T}{2E_\mathrm{f}}(L_\uparrow^2 + L_\downarrow^2) - u_\mathrm{m}(L_\downarrow) - u_\mathrm{m}(L_\uparrow) \tag{A.36}$$

so that the fiber crack bridge function becomes

$$\varepsilon_{\mathrm{f0},\mathbf{X}}(w, \mathbf{X}) = \frac{w + T(L_\uparrow^2 + L_\downarrow^2)/(2E_\mathrm{f}) + u_\mathrm{m}(L_\downarrow) + u_\mathrm{m}(L_\uparrow)}{(L_\uparrow + L_\downarrow)}. \tag{A.37}$$

The matrix displacements $u_\mathrm{m}(L)$ are defined by integrating the matrix strain given by Eq. (A.8)

$$u_\mathrm{m}(L) = \int_{-\infty}^{\varepsilon'_{\mathrm{f},L,\mathbf{X}}} \varepsilon_\mathrm{m}(\varepsilon'_{\mathrm{f},\mathbf{X}}) \frac{\mathrm{d}a}{\mathrm{d}\varepsilon'_{\mathrm{f},\mathbf{X}}} \mathrm{d}\varepsilon'_{\mathrm{f},\mathbf{X}}, \tag{A.38}$$

where the differential $\mathrm{d}a/\mathrm{d}\varepsilon'_{\mathrm{f},\mathbf{X}}$ is a piecewise function given by Eqns. (A.12) and (A.28) for the respective ranges of the debonded lengths $a < L_\downarrow$ and $a > L_\downarrow$. The integration limit $\varepsilon'_{\mathrm{f},L,\mathbf{X}}$ is the value of the fiber strain derivative $\varepsilon'_{\mathrm{f},\mathbf{X}}$, which solves Eq. (A.25) for $a(\varepsilon'_{\mathrm{f},\mathbf{X}}) = L_\downarrow$ or Eq. (A.35) for $a_\uparrow(\varepsilon'_{\mathrm{f},\mathbf{X}}) = L_\uparrow$ for the respective evaluations of either $u_\mathrm{m}(L_\downarrow)$ or $u_\mathrm{m}(L_\uparrow)$.

References

[1] Ahn BK, Curtin WA. Strain and hysteresis by stochastic matrix cracking in ceramic matrix composites. J Mech Phys Solids 1997;45(2):177–209.
[2] Aveston J, Cooper G, Kelly A. Single and multiple fracture, the properties of fibre composites. Proc. Conf. National physical laboratories. London: IPC Science and Technology Press Ltd; 1971. p. 15–24.
[3] Aveston J, Kelly A. Theory of multiple fracture of fibrous composites. J Mat Sci 1973;8:411–61.
[4] Banerjee S, Sankar BV. Mechanical properties of hybrid composites using finite element method based micromechanics. Compos Part B Eng 2014;58:318–27.
[5] Bažant ZP, Planas J. Fracture and size effect in concrete and other quasibrittle materials. Taylor & Francis; 1997.
[6] Budiansky B, Hutchinson JW, Evans AG. Matrix fracture in fiber-reinforced ceramics. J Mech Phys Solids 1986;34(2):167–89.
[7] Butler M, Hempel S, Mechtcherine V. Modelling of ageing effects on crack-bridging behaviour of AR-glass multifilament yarns embedded in cement-based matrix. Cem Concr Res 2011;41(4):403–11.
[8] Caggiano A, Etse G, Martinelli E. Zero-thickness interface model formulation for failure behavior of fiber-reinforced cementitious composites. Comput Struct 2012;98:23–32.
[9] Chiang Y-C, Wang ASD, Chou T-W. On matrix cracking in fiber reinforced ceramics. J Mech Phys Solids 1993;41(7):1137–54.
[10] Choi BK, Yoon GH, Lee S. Molecular dynamics studies of cnt-reinforced aluminum composites under uniaxial tensile loading. Compos Part B Eng 2016;91:119–25.
[11] Choi W-C, Jang S-J, Yun H-D. Interface bond characterization between fiber and cementitious matrix. Int J Polym Sci 2015;1–11:2015.
[12] Chudoba R, Sadílek V, Rypl R, Vořechovský M. Using python for scientific computing: efficient and flexible evaluation of the statistical characteristics of functions with multivariate random inputs. Comput Phys Commun 2013;184(2):414–27.
[13] Chudoba R, Vořechovský M, Eckers V, Gries Th. Effect of twist, fineness, loading rate and length on tensile behavior of multifilament yarns (a multivariate study). Text Res J 2007;77(11):880–91.
[14] Chudoba R, Vořechovský M, Konrad M. Stochastic modeling of multifilament yarns. I. random properties within the cross-section and size effect. Int J Solids Struct 2006;43(3–4):413–34.
[15] Chudoba R, Vořechovský M, Rypl R. Identification of the effective bundle length in a multifilament yarn from the size effect response. J Compos Mater 2011;45(25):2659–68.
[16] Claramunt J, Ventura H, Fernndez-Carrasco LJ, Ardanuy M. Tensile and flexural properties of cement composites reinforced with flax nonwoven fabrics. Materials 2017;10(2):215.
[17] Cox HL. The elasticity and strength of paper and other fibrous materials. Br J Appl Phys 1952;3:72–9.
[18] Curtin WA. Exact theory of fiber fragmentation in a single-filament composite. J

Mater Sci 1991;26:5239–53.
[19] Curtin WA. The tough to brittle transition in brittle matrix composites. J Mech Phys Solids 1993;41(2):217–45.
[20] Curtin WA. Stochastic damage evolution and failure in fiber-reinforced composites. Adv Appl Mech 1999;36(36):163–253.
[21] Curtin WA, Ahn BK, Takeda N. Modeling brittle and tough stress-strain behavior in unidirectional ceramic matrix composites. Acta mater 1998;46(10):3409–20.
[22] Curtin WA, Olmsted DL. A predictive mechanism for dynamic strain ageing in aluminium-magnesium alloys. Nat Mater 2006;5(11):875–80.
[23] Daniels HE. The statistical theory of the strength of bundles of threads. I Proc R Soc Lond Ser A, Math Phys Sci 1945;183(995):405–35.
[24] Donnini J, Corinaldesi V, Nanni A. Mechanical properties of FRCM using carbon fabrics with different coating treatments. Compos Part B Eng 2016;88:220–8.
[25] Dvorak GJ, Šejnoha M. Initial failure maps for fibrous SMC laminates. J Am Ceram Soc 1995;78:205–10.
[26] Dvorak GJ, Šejnoha M. Initial failure maps for ceramic and metal matrix composites. Model Simul Mater Sci Eng 1996;4:553–80.
[27] Dvorak GJ, Šejnoha M, Srinivas M. Pseudoplasticity of fibrous composite materials: inelastic response of laminates with interfacial decohesion. In: Pineau A, Zaoui A, editors. IUTAM symposium on micromechanics of plasticity and damage of multiphase materials: proceedings of the IUTAM symposium held in sèvres, paris, France, 29 August – 1 September 1995. Springer Netherlands: Springer; 1996. p. 43–50. volume 46 of Solid Mechanics and its Applications.
[28] Evans AG, Zok FW. The physics and mechanics of fiber-reinforced brittle-matrix composites. J Mater Sci 1994;29(15):3857–96.
[29] Fantilli AP, Mihashi H, Vallini P. Multiple cracking and strain hardening in fiber reinforced concrete under uniaxial tension. Cem Concr Res 2009;39:1217–29.
[30] Fereidoon A, Rajabpour M, Hemmatian H. Fracture analysis of epoxy/SWCNT nanocomposite based on globallocal finite element model. Compos Part B Eng 2013;54:400–8.
[31] Greco A, Maffezzoli A, Casciaro G, Caretto F. Mechanical properties of basalt fibers and their adhesion to polypropylene matrices. Compos Part B Eng 2014;67:233–8.
[32] Harlow DG, Smith RL, Taylor HM. Lower tail analysis of the distribution of the strength of load-sharing systems. J Appl Probab 1983;20(2):358–67.
[33] Hegger J, Horstmann M, Voss S, Will N. Textile reinforced concrete load-bearing behaviour, design and application. Beton- Stahlbetonbau 2007;102(6):362–70.
[34] Henstenburg RB, Phoenix SL. Interfacial shear strength studies using the single-filament-composite test. part II: a probability model and Monte Carlo simulation. Polym Compos 1989;10(5):389–408.
[35] Ibnabdeljalil M, Curtin WA. Strength and reliability of fiber-reinforced composites: localized load-sharing and associated size effects. Int J Solids Struct 1997;34(21):2649–68.
[36] Khan Z, Yousif BF, Islam M. Fracture behaviour of bamboo fiber reinforced epoxy composites. Compos Part B Eng 2017;116:186–99.
[37] Konrad M, Chudoba R. Tensile behavior of cementitious composite reinforced with epoxy impregnated multifilament yarns. Int J Multiscale Eng 2009;7(2):115–33.
[38] Koo B, Subramanian N, Chattopadhyay A. Molecular dynamics study of brittle fracture in epoxy-based thermoset polymer. Compos Part B Eng 2016;95:433–9.
[39] Li Y, Bielak J, Hegger J, and Chudoba R. An incremental inverse analysis procedure for the identification of bond-slip laws in composites applied to textile reinforced concrete. Composites Part B: Engineering, in review; minor revision.
[40] Di Maida P, Radi E, Sciancalepore C, Bondioli F. Pullout behavior of polypropylene macro-synthetic fibers treated with nano-silica. Constr Build Mater 2015;82:39–44.
[41] Marshall DB, Cox BN, Evans AG. The mechanics of matrix cracking in brittle-matrix fiber composites. Acta Metall 1985;33(11):2013–21.
[42] Marshall DB, Evans AG. Failure mechanisms in ceramic-fiber ceramic-matrix composites. J Am Ceram Soc 1985;68(5).
[43] Meda G, Steif PS. A detailed analysis of cracks bridged by fibersI. limiting cases of short and long cracks. J Mech Phys Solids 1994;42(8):1293–321.
[44] Meda G, Steif PS. Cracks bridged by fibersII. cracks of intermediate size. J Mech Phys Solids 1994;42(8):1323–41.
[45] Mobasher B, Pahilajani J, Peled A. Analytical simulation of tensile response of fabric reinforced cement based composites. Cem Concr Compos 2006;28(1):77–89.
[46] Nair AK, Warner DH, Hennig RG, Curtin WA. Coupling quantum and continuum scales to predict crack tip dislocation nucleation. Scr Mater 2010;63(12):1212–5.
[47] Nairn JA. On the use of shear-lag methods for analysis of stress transfer in unidirectional composites. Mech Mater 1997;26(2):63–80.
[48] Okabe T, Takeda N, Kamoshida Y, Shimizu M, Curtin WA. A 3D shear-lag model considering micro-damage and statistical strength prediction of unidirectional fiber-reinforced composites. Compos Sci Technol 2001;61(12):1773–87.
[49] Phoenix SL. Probabilistic strength analysis of fibre bundle structures. Fibre Sci Technol 1974;7:15–30.
[50] Phoenix SL, Raj R. Scalings in fracture probabilities for a brittle matrix fiber composite. Acta Metallurgica Mater. 1992;40(11):2813–28.
[51] Procházka P, Šejnoha M. Development of debond region of lag model. Comput Struct 1995;55(2):249–60.
[52] Radi E, Lanzoni L, Sorzia A. Analytical modelling of the pullout behavior of synthetic fibres treated with nano-silica. Procedia Eng 2015;109:525–32. XXIII Italian Group of Fracture Meeting, IGFXXIII.
[53] Rypl R. Probabilistic approach to the mechanics of composites with heterogeneous reinforcement PhD thesis RWTH Aachen University; 2014
[54] Rypl R, Chudoba R, Mörschel U, Stapleton SE, Gries T, Sommer G. A novel tensile test device for effective testing of high-modulus multi-filament yarns. J Ind. Text 2015;44(6):934–47.
[55] Rypl R, Chudoba R, Scholzen A, Vořechovský M. Brittle matrix composites with heterogeneous reinforcement: multi-scale model of a crack bridge with rigid matrix. Compos Sci Technol 2013;89:98–109.
[56] Rypl R, Chudoba R, Vořechovský M. On the strength of composites with heterogeneous reinforcement, Copenhagen, Denmark. ICCM20 – 20th international conference on composite materials. 2015. p. 1–12. paper ID 3214–3.
[57] Scholzen A, Chudoba R, Hegger J. Thin-walled shell structure made of textile reinforced concrete: design, dimensioning and realization. Beton- Stahlbetonbau 2012;107(11):767–75.
[58] Smith RL, Phoenix SL, Greenfield MR, Henstenburg RB, Pitt RE. Lower-tail approximations for the probability of failure of three-dimensional fibrous composites with hexagonal geometry. Proc R Soc Lond Ser A, Math Phys Sci 1983;388(1795):353–91.
[59] Song J, Curtin WA. Atomic mechanism and prediction of hydrogen embrittlement in iron. Nat Mater 2013;12(2):145–51.
[60] Thouless M, Evans A. Effects of pull-out on the mechanical-properties of ceramic-matrix composites. Acta Metall 1988;36(3):517–22.
[61] Vořechovský M, Chudoba R. Stochastic modeling of multifilament yarns: II. random properties over the length and size effect. Int J Solids Struct 2006;43(3–4):435–58.
[62] Weichold O, Hojczyk M. Size effects in multifilament glass-rovings: the influence of geometrical factors on their performance in textile-reinforced concrete. Text Res J 2009;79(16):1438–45.
[63] Xia Z, Curtin WA. Tough-to-brittle transitions in ceramic-matrix composites with increasing interfacial shear stress. Acta Mater 2000;48(20):4879–92.
[64] Xia Z, Curtin WA, Okabe T. Green's function vs. shear-lag models of damage and failure in fiber composites. Compos Sci Technol 2002;62(10–11):1279–88.
[65] Xia Z, Curtin WA, Peters PWM. Multiscale modeling of failure in metal matrix composites. Acta Mater 2001;49(2):273–87.
[66] Xia Z, Okabe T, Curtin WA. Shear-lag versus finite element models for stress transfer in fiber-reinforced composites. Compos Sci Technol 2002;62(9):1141–9.
[67] Xia ZH, Curtin WA. Multiscale modeling of damage and failure in aluminum-matrix composites. Compos Sci Technol 2001;61(15):2247–57.
[68] Yamakov VI, Warner DH, Zamora RJ, Saether E, Curtin WA, Glaessgen EH. Investigation of crack tip dislocation emission in aluminum using multiscale molecular dynamics simulation and continuum modeling. J Mech Phys Solids 2014;65(0):35–53.
[69] Yu Y, Zhang B, Tang Z, Qi G. Stress transfer analysis of unidirectional composites with randomly distributed fibers using finite element method. Compos Part B Eng 2015;69:278–85.
[70] Zhandarov S, Mäder E. Characterization of fiber/matrix interface strength: applicability of different tests, approaches and parameters. Compos Sci Technol 2005;65(1):149–60.
[71] Zhao L, Li Y, Zhang J, Zhou L, Hu N. A novel material degradation model for unidirectional cfrp composites. Compos Part B Eng 2018;135:84–94.